



Contents lists available at ScienceDirect

## Chemical Engineering Journal

journal homepage: [www.elsevier.com/locate/cej](http://www.elsevier.com/locate/cej)

# Hybrid architectures based on noble metals and carbon-based dots nanomaterials: A review of recent progress in synthesis and applications

Yukui Fu<sup>a,b</sup>, Guangming Zeng<sup>a,b,\*</sup>, Cui Lai<sup>a,b,\*</sup>, Danlian Huang<sup>a,b,\*</sup>, Lei Qin<sup>a,b</sup>, Huan Yi<sup>a,b</sup>,  
Xigui Liu<sup>a,b</sup>, Mingming Zhang<sup>a,b</sup>, Bisheng Li<sup>a,b</sup>, Shiyu Liu<sup>a,b</sup>, Ling Li<sup>a,b</sup>, Minfang Li<sup>a,b</sup>,  
Wenjun Wang<sup>a,b</sup>, Yujin Zhang<sup>a,b</sup>, Zhoujie Pi<sup>a,b</sup>

<sup>a</sup> College of Environmental Science and Engineering, Hunan University, Changsha 410082, PR China

<sup>b</sup> Key Laboratory of Environmental Biology and Pollution Control, Hunan University, Ministry of Education, Changsha 410082, PR China

## HIGHLIGHTS

- The synthetic methods of NMs/CDs mainly include chemical reduction, hydrothermal method and assembled method.
- The combination of NMs and CDs synergizes their respective strengths for enhanced performance.
- The electronic properties and up-conversion ability of CDs, as well as LSPR effect of NMs boost the catalytic performance.
- Each NMs/CDs in different application has its own characteristic depending on the applied conditions.

## GRAPHICAL ABSTRACT



## ARTICLE INFO

## Keywords:

Carbon-based dots  
Noble metals  
Hybrid architectures fabrication  
Pollutants treatment and detection  
Energy production

## ABSTRACT

Recently, hybrid architectures are extensively developed in environment and energy field with outstanding and multifunctional property to make up the drawbacks of “less efficient” single-component nanomaterials. Thereinto, noble metals (NMs) are rationally integrated with carbon-based dots (CDs) as one of the most commonly pursued nanohybrids, which can synergize their respective strengths after combining properties such as electronic property, up-conversion ability and localized surface plasmon resonance (LSPR) and exhibit enhanced features in the diverse applications. Herein, this review focuses on the synthetic methods, physico-chemical characterizations and recent progress in applications of noble metal/carbon dots nanohybrids (NMs/CDs). Specifically, (i) synthetic methods of NMs/CDs nanohybrids are concluded, which are different from the synthetic methods of NMs or CDs single component and have not been systematically concluded. It can help guide the NMs/CDs nanohybrids control synthesis for obtaining target materials accordingly. (ii) physico-chemical characterizations of NMs/CDs nanohybrids are briefly summarized. (iii) applications of NMs/CDs nanohybrids in environment field (pollutants detection and treatment) and energy field (water splitting, oxygen reduction reaction and methanol oxidation reaction) are summarized. In particular, the mechanisms and synergistic effect between the two components in these applications are emphasized. Finally, the limitation and prospects of NMs/CDs in remaining issues are proposed for further development of these nanohybrids.

\* Corresponding authors at: College of Environmental Science and Engineering, Hunan University, Changsha 410082, PR China.

E-mail addresses: [zgming@hnu.edu.cn](mailto:zgming@hnu.edu.cn) (G. Zeng), [laicui@hnu.edu.cn](mailto:laicui@hnu.edu.cn) (C. Lai), [huangdanlian@hnu.edu.cn](mailto:huangdanlian@hnu.edu.cn) (D. Huang).

<https://doi.org/10.1016/j.cej.2020.125743>

Received 7 January 2020; Received in revised form 28 May 2020; Accepted 1 June 2020

Available online 04 June 2020

1385-8947/ © 2020 Elsevier B.V. All rights reserved.

## 1. Introduction

The adverse environment and energy problems have attracted a lot of attention, leading to an ever-increasing need to develop multifunctional materials with enhanced and/or essential properties to address these problems [1]. Noble metals (NMs) nanoparticles have emerged as a class of materials in many applications on account of their unique electronic and optical properties [2]. Especially, the NMs can be applied in photocatalysis field under visible light irradiation owing to the localized surface plasmon resonance (LSPR) excitation, which is caused by collective oscillations of free electrons driven by the electromagnetic field of incident light [3,4]. As is well known, the catalytic activity of NMs is directly related to their particle size and dispersivity [5,6]. As single-component nanostructures, NMs would suffer serious aggregation on account of high surface energy, resulting in the change of particle size and decrease of single-component NMs dispersivity. It may cause NMs insufficient to maintain adequate catalytic efficiency in environmental pollutants removal and energy conversion [4,7]. Hence, various efforts have been attempted to impede the aggregation of NMs and obtain better catalytic efficiency [8,9]. Among them, rational integration of NMs and other nanomaterials, such as immobilization of NMs onto materials and confinement of NMs into materials forming core-shell structure, has attracted research interest. It not only prevents the aggregation of NMs, but also combines the properties of both NMs and other nanomaterials with several advantages over single-component materials [10].

Carbon-based nanomaterials including carbon nanotubes, graphene family materials, and recently, emerging materials carbon-based dots possess good properties of chemical stability, electrical conductivity and availability [10–14], which have been used as ideal materials for combining with NMs or transition metals, transition metal oxides et al [15–18]. Especially, carbon-based dots (CDs) such as carbon dots (C-dots) and carbon/graphene quantum dots (GQDs or CQDs) with abundant functional groups, super conductivity and excellent photostability have been used to integrate with NMs to effectively disperse NMs and obtain multiple benefits [10,19–31]. Firstly, during synthesis of NMs/CDs nanohybrids, CDs with abundant oxygen-containing functional groups, such as carboxyl and hydroxyl groups (–COOH and –OH), could prevent NMs from aggregation and ensure the activity of NMs by engineering the properties such as size of NMs [32–36], since the size of NMs are crucial for activity in the design hybrids [37–40]. Secondly, the hybridized NMs also facilitate the realization of high dispersivity of CDs. Moreover, the tunable optoelectronic property and excellent up-conversion ability of CDs, as well as LSPR excitation of NMs that display LSPR bands located in visible and/or near-infrared (NIR) region, can maximize utilization of solar energy in full spectrum and thereby broaden the scope of NMs/CDs nanohybrids in many applications such as plasmonic photocatalysis and plasmon-enhanced fluorescence [3,41–45]. Most notably, the superior electronic properties of both CDs and NMs can facilitate electron transfer, resulting in restricting charge carrier recombination by ultrafast relaxation process of LSPR induced hot electrons [5,11,46–49], which can boost the performances toward more effective energy environmental sensing, pollutants treatment and energy conversion [50]. Hence, integrating CDs with NMs plays an active part in making the best of the excellent nature of the two components, yielding a synergistic effect and exhibiting enhanced features in the applications of sensing and catalysis [51–53].

In the past few years, many works have been done to hybridize NMs with carbon-based materials to enhance their performance in various applications. A number of reviews have reported NMs hybridized with carbon-based materials (including graphene, carbon nanotube, and carbon nitrides, and CDs) in their synthetic methods, properties and applications [10,25–27,47,54]. For instance, Wang et al. have summarized different carbon-based materials hybridized with metal/metal oxide nanoparticles, and briefly introduces the synthetic methods and how the carbon-based materials hybridized with metal/metal oxide

nanoparticles exhibit altered and emerging attributes and their applications in energy, water and the environment [10]. However, there are few reviews focusing on NMs hybridized with CDs-based materials, systematically summarizing the fabrication of NMs/CDs nanohybrids and comparing the differences between the various methods. In addition, the applications in environment-related and energy-related fields of NMs/CDs were rarely summed up. Hence, considering the integrating CDs with NMs for new or enhanced properties has been extensively studied in recent years, we summarize the synthetic methods, physicochemical characterizations and the applications of NMs/CDs nanohybrids in environment-related field (pollutants detection and treatment) and energy-related field (water splitting, oxygen reduction reaction and methanol oxidation reaction). Thereinto, the synthetic methods of NMs/CDs nanohybrids can help guide the NMs/CDs nanohybrids controlled synthesis for obtaining target materials accordingly, which are different from the synthetic methods of NMs or CDs single component and have not been systematically summarized. In addition, the synergistic effect of NMs/CDs and how NMs/CDs can realize improved properties in diverse applications are discussed to better reveal the mechanism. The limitations and challenges are also indicated to discriminate future research strategies for this category of nanohybrids.

## 2. Fabrication of NMs/CDs nanohybrids

According to the literatures, there are diverse synthetic methods for NMs/CDs [55,56]. In this section, the detailed discussion of the available synthetic methods of NMs/CDs is summarized. In general, the synthetic methods of NMs/CDs mainly include chemical reduction, hydrothermal method and assembled method, each providing different degrees of controlling for the size and distribution of NMs and CDs (Table 1). Under a chemical reduction, NMs intend to grow onto CDs surface owing to the abundant oxygen-containing groups of CDs, which can promote the formation of NMs by chemical reduction pathways (Fig. 1A) [57]. It may lead to a core-shell (CDs-NMs) structure. For instance, a shell of Ag was formed on the surface of CDs via chemical reduction pathways, which was confirmed by TEM (Fig. 1B). On the contrary, under hydrothermal method and electrostatic assembled method, CDs mostly prefer to deposit onto NMs surface, forming a “dot on particles” structure (Fig. 1C and D) [39,58]. Commonly, NMs with small diameter could be obtained by using hydrothermal method. The comparison of these methods in terms of advantages, disadvantages and synthesis processes has been summarized in Table 1.

### 2.1. Chemical reduction method

Chemical reduction is a conventional method for the synthesis of NMs/CDs nanohybrids. Generally, the CDs are firstly synthesized via “Top-Down” or “Bottom-Up” approaches before the chemical reduction to prepare NMs/CDs [59,60]. Then, the as-prepared CDs, metal precursors and reduction agent are added into a solution to conduct chemical reduction. As for the reduction of metal precursors, various chemical agents such as borohydride [61,62] and trisodium citrate [39,63,64] serve as reduction agents in the synthesis of NMs/CDs. Despite metal precursors could be easily reduced to metallic nanoparticles (NPs), this method requires hazardous chemicals and easily introduces some by-products. For example, Tesfalidet Balcha et al. synthesized AuPd core-shell structure by the sequential reduction method using sodium borohydride and ascorbic acid (AA). However, in order to remove the excess salts and AA, the NPs had to dialyze overnight. Hence, a number of studies have been centered on the green and facile chemical methods for NMs/CDs synthesis.

Considering the excellent electron donation ability, CDs could accelerate the electron transfer rate to metal precursors and have promising potential to function as reduction agent [65–68]. Many studies have used CDs as mild reduction agent to reduce metal precursors without any additional reducing agent to realize a well dispersivity of

**Table 1**  
The synthetic methods of NMs/CDs hybrids and corresponding average size of NMs.

Synthetic methods	Advantages	Disadvantages	Hybrids	Synthetic process	NMs size (nm)	Ref.
Chemical reduction	(i) Short preparation time;(ii) Simple equipment requirements;(iii) Room temperature and normal pressure reaction condition;(iv) Suitable cost.	(i) Poor control to size of NMs;(ii) Environment pollution.	Au-CQDs Ag-CQDs AuAg@Carbon nanodots AuNPs/r-CDs r-CD/Pt	(i) CQDs were produced by incompletely pyrolyzing citric acid;(ii) H <sub>2</sub> SO <sub>4</sub> mixed CQDs solution was heat to boiling followed by adding trisodium citrate as reducing agent. (i) CQDs were prepared through electrochemical approach;(ii) AgNO <sub>3</sub> was added into CQDs with stirring under UV irradiation. (i) C-dots were prepared by thermal degradation of solid citric acid;(ii) H <sub>2</sub> SO <sub>4</sub> and AgNO <sub>3</sub> were sequentially added to the hot C-dots (100 °C) followed by reacting for 15 min. (i) C-dots were produced by “oil-bath” strategy using sucrose as the carbon source;(ii) H <sub>2</sub> SO <sub>4</sub> was directly added into r-CDs solution under room temperature. (i) CQDs were prepared via a solvothermal method from citric acid and urea using DMF as solvent. (ii) H <sub>2</sub> SO <sub>4</sub> and CQDs were mixed for 24 h at room temperature.	15.00 28.00 5.60 15.00 4.00–8.00	[64] [74] [117] [68] [23]
Hydrothermal method	(i) Simple operation process;(ii) Uniformity of the reaction system;(iii) Effective cost.(iv) Environmental friendliness.	(i) Long reaction time;(ii) High pressure and temperature reaction condition;(iii) Dependent on reaction equipment.	Au-SCQDs Au/N-CQDs Ru@CQDs	N-(2-hydroxybenzyl)-cysteine mixed with H <sub>2</sub> SO <sub>4</sub> were transferred into autoclave and heated at 180 °C for 12 h. Folic acid, Glycerol, and H <sub>2</sub> SO <sub>4</sub> were dissolved in water under heating agitator at 80 °C for 10 min, and then transferred into autoclave and heated at 180 °C for 12 h. (i) The CQDs were firstly synthesized by a hydrothermal method;(ii) RuCl <sub>3</sub> was dissolved in CQDs solution and then the mixture were transferred to an autoclave at 200 °C for 8 h.	– 4.01 3.28	[83] [85] [86]
Assembled method	(i) Mild reaction conditions;(ii) Less pollution.	(i) Difficulty on a large scale production.(ii) Complicated pre-synthetic process.	(M/GQDs) <sub>n</sub> (M = Au, Ag, Pt) Au/GQDs/ NP-TNTAs(nanoporous TiO <sub>2</sub> nanotube arrays)	(i) Negatively charged M NPs were prepared by citrate-stabilized method and positively charged GQDs were prepared with CX-72 carbon black via reflux method;(ii) The as-prepared M NPs and GQDs were deposited on the fluorine-doped tin oxide with varying assembly cycles through electrostatic interaction. (i) Positively charged NP-TNTAs and negatively charged colloidal GO quantum occur the electrostatic assembly followed by calcination in an inert atmosphere to obtain GQDs/nanoporous TiO <sub>2</sub> nanotube arrays.(ii) GQDs/NP-TNTAs were treated with aminopropyltrimethoxysilane (APTMS) to obtain a positively charged surface.(iii) Positively charged GQDs/NP-TNTAs combines with negatively charged Au clusters via the electrostatic assembly.	14.2; 6.47; 3.09 1.5	[39] [56]

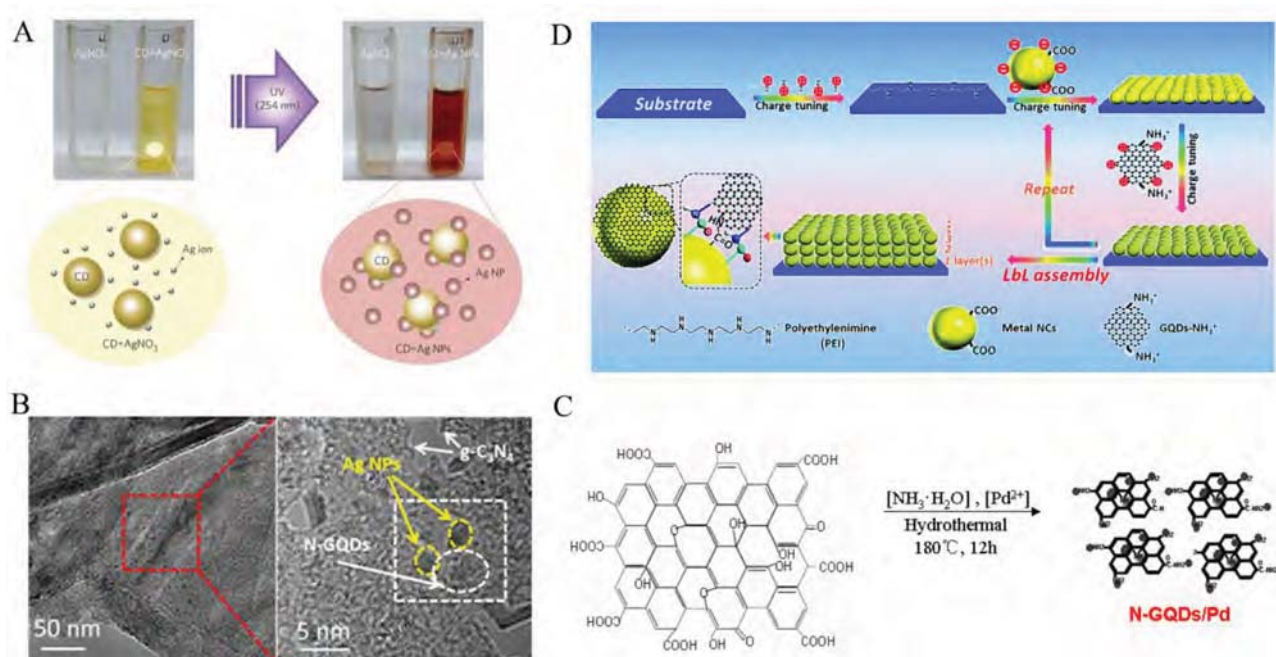


**Fig. 1.** Reported synthetic methods of NMs/CDs nanohybrids: (A) Chemical reduction method. Reprinted from Ref. [57] with permission from Nature. (B) TEM and HRTEM images of Ag/N-GQDs/g-C<sub>3</sub>N<sub>4</sub>. Reprinted from Ref. [52] with permission from American Chemical Society. (C) Hydrothermal method. Reprinted from Ref. [58] with permission from Elsevier. (D) Assembled method. Reprinted from Ref. [39] with permission from Royal Society of Chemistry.

MNPs [19,22,69–71]. The method proved as a green and facile method for NMs/CDs synthesis [72]. For instance, Luo et al. constructed silver/graphene quantum dots (Ag/CQDs) composites using CQDs as reduction agent [73]. They prepared amide and aldehyde-rich CQDs via hydrothermal method firstly, and mixed the CQDs and AgNO<sub>3</sub> under the conditions of vigorous stirring at 90 °C. Li et al. synthesized GQDs using an electrochemical method with abundant –OH, –COOH, and –C = O groups on CDs surfaces. Then, the as-prepared GQDs were used to reduce Ag<sup>+</sup> to Ag NPs with ultraviolet (UV) irradiation [74]. Kirillov et al. also used CDs as reduction agent to reduce Ag<sup>+</sup> to Ag NPs onto the surface of magnesium–aluminum layered double hydroxide support doped with Ce (Mg–Al–Ce-LDH) matrix under UV irradiation [70]. Here, CDs donated electrons under UV light irradiation, and the photo-induced electrons rapidly facilitated the formation of Ag NPs. Furthermore, the abundant oxygen-containing functional groups (–OH, –COOH, –C = O) on CDs surface is conducive to reduce Ag<sup>+</sup> to Ag NPs and enhance the stability of Ag NPs in a water-based environment.

In above reported methods, external energy such as heating, photon or microwave irradiation is needed for CDs as a reduction agent [23,75–79]. In order to simplify the synthesized method of NMs/CDs, direct method without adding external energy by simply mixing CDs with metal precursors has been proposed [80,81]. Zhang et al. constructed CDs/Au NPs through simply mixing CDs and HAuCl<sub>4</sub> at room temperature [40,82]. This method involves the preparation of hydroxyl-rich CDs via a one-pot electrochemical carbonization of ethylene glycol firstly, and the CDs mixed with chloroauric acid (HAuCl<sub>4</sub>) followed by incubated at room temperature for 20 min without further processing and external energy. Xiao et al. has reported a fast strategy for surfactant-free Au NPs synthesis using reductive CDs [68]. During the preparation, Au NPs were rapidly formed only within 30 s at room temperature, ascribed to the high reducibility of carbon dots (r-CDs). According to the above-mentioned reports, it can be concluded that the remarkable reduction property of CDs is related to electron donation ability and the nature of surface functional groups, such as –OH, –COOH, –C = O, confirmed by Liu et al [65]. They used KMnO<sub>4</sub> to oxidize hydroxyl groups on CDs surface and found that the HAuCl<sub>4</sub> could not be reduced by the treated CDs with KMnO<sub>4</sub>, thereby

illustrating that the functional groups on CDs play an important part in the reducibility [22,51,73,74].

## 2.2. Hydrothermal method

Hydrothermal synthesis method can be considered as an environment friendly method with simple operations and is used to synthesize NMs/CDs nanohybrids [55,83,84]. For instance, Li et al. synthesized Au and N co-doped CQDs (Au/N-CQDs) using a one-step hydrothermal method at 180 °C for 12 h, with folic acid as carbon and nitrogen source, glycerol as carbon source and HAuCl<sub>4</sub> as gold source [85]. The average diameter of as-prepared Au/N-CQDs was 4.01 ± 1 nm. Similarly, a well-dispersed N-doped GQDs-supported Pd (N-GQDs/Pd) was also synthesized via facile hydrothermal method, in which the diameter of Pd was 4.8 ± 0.2 nm [58]. Recently, Liu et al. used two-step hydrothermal method to synthesize Ru@CQDs [86]. CQDs were firstly synthesized by a typical hydrothermal method, and then mixed with RuCl<sub>3</sub> using hydrothermal method at 200 °C for 8 h to synthesize Ru@CQDs. The Ru NPs with a diameter of 3.28 nm were well dispersed in the CQDs matrix.

## 2.3. Assembled method

Assembled method takes advantages of the interaction of materials with complementary functional groups such as electrostatic interaction, hydrogen bonding or other intermolecular interactions [39,56,87]. For instance, Shan et al. assembled CQDs/Au nanoclusters (CQDs/Au NCs) via a carbodiimide-activated coupling reaction [88]. They firstly synthesized CQDs by a modified hydrothermal method followed by coating with (3-aminopropyl)triethoxysilane (APTES), and then synthesized Au NCs capped by 11-mercaptopundecanoic acid (MUA) by a chemical reduction. The –NH<sub>2</sub> groups on CQDs surface and –COOH on Au NCs surface would interact via carbodiimide-activated coupling reaction, resulting the assembly of CQDs and Au NCs. Recently, Zeng et al. designed a layer-by-layer assembly method to directly assemble the as-prepared positively-charged CQDs and negatively-charged Au, Ag or Pt NCs [39]. This assembled method was based on pronounced



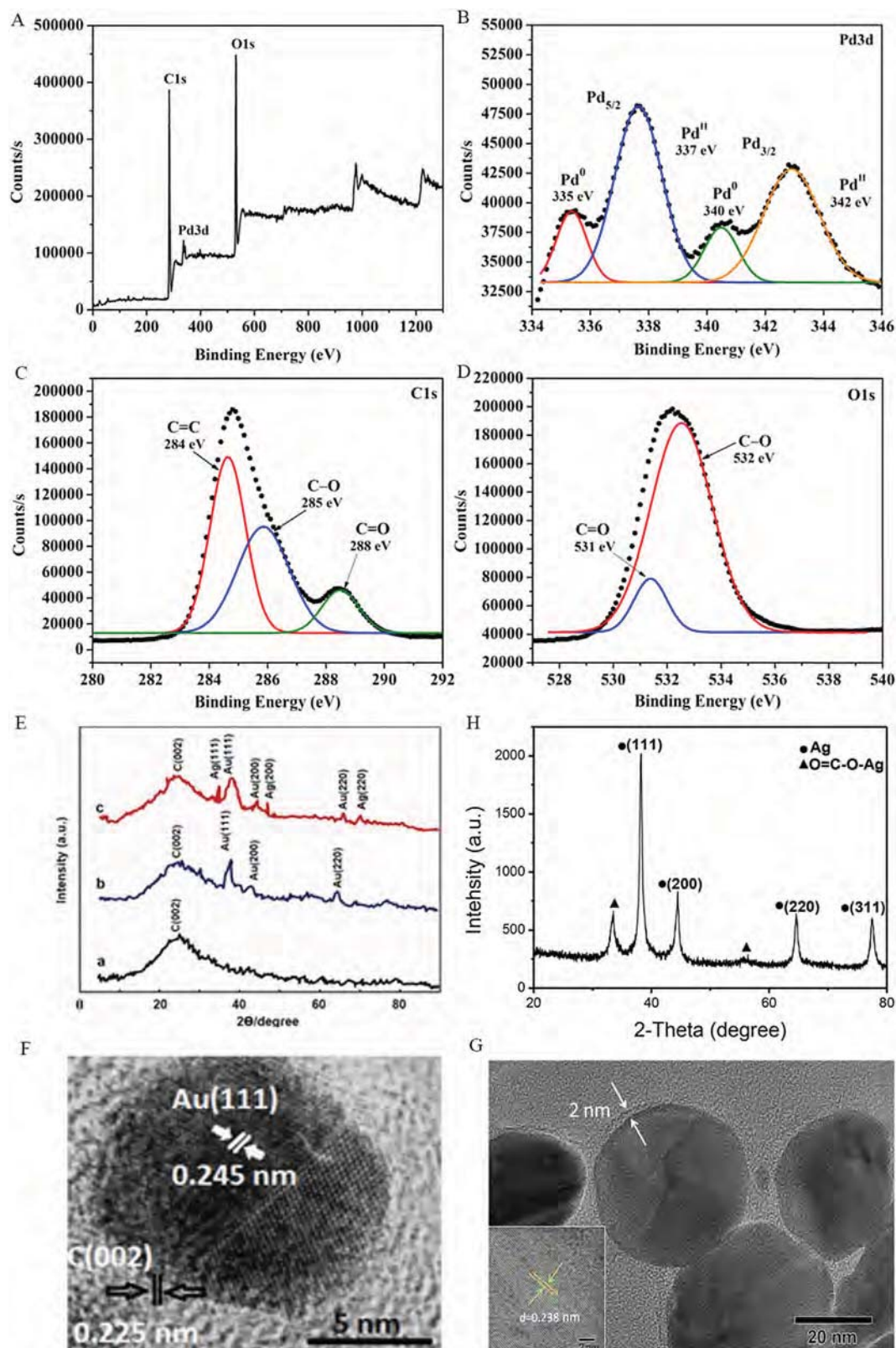


**Fig. 2.** (A) XPS survey spectrum and deconvoluted high-resolution XPS images of (B) Pd 3d, (C) C 1s, and (D) O 1s of Pd@RCD nanohybrid. Reprinted from Ref. [89] with permission from American Chemical Society. (E) XRD patterns and (F) HRTEM of Au NPs@NCDS@Ag NPs. Reprinted from Ref. [92] with permission from Electrochemical Society, Inc. (G) HRTEM and (H) XRD patterns of Ag@CD NPs. Reprinted from Ref. [91] with permission from American Chemical Society.

electrostatic attractive interaction, which simplified the synthesized process and provided more intimate interfacial contact among CQDs and NMs [56].

### 3. Physicochemical characterization of NMs/CDs nanohybrids

#### 3.1. Surface chemistry characterization

X-ray photoelectron spectroscopy (XPS) is often used as a laboratory tool in material characterization. As for NMs/CDs hybrids, XPS analysis can provide some information about the composition of the elements and the character of functional groups. For instance, as displayed in the XPS analysis of Pd@reduced carbon dots (Pd@RCD) nanohybrid (Fig. 2A), the surface survey spectrum displayed the three peaks corresponding to C 1s, Pd 3d and O 1s, ascertaining the presence of these elements in Pd@RCD [89]. As shown in Fig. 2B, the deconvoluted high-resolution of Pd 3d showed two sets of doublets, confirming the presence of Pd<sup>0</sup> and Pd<sup>2+</sup>. The deconvoluted high-resolution of C 1s and O 1s (Fig. 2C and D) revealed the abundant oxygenous surface functional groups in RCD. In another work, XPS analysis was employed to investigate the interaction between Au NPs and the functional groups on the poly(N-isopropylacrylamide) (PNIPAM) functionalized carbon dots (CD@P) [90,91]. They found that a tiny shift occurred in the Au 4f7/2 and Au 4f5/2 to higher energy, ascribed to efficient electrons transfer from the CD/CD@P to the Au NPs.

The crystalline structure of NMs/CDs nanohybrids have been investigated by X-Ray diffraction spectroscopy (XRD) and high-resolution transmission electron microscopy (HRTEM). As for Au NPs@NCDS@Ag NPs composites, Au NPs and Ag NPs in the composites displayed characteristic diffraction peaks in XRD patterns, corresponding to specific lattice plane (Fig. 2E), and displayed a distance of 0.245 nm with (1 1 1) plane of Au NPs, as reflected in HRTEM images (Fig. 2F) [92]. And CDs in the composites displayed a broad peak near 25° in XRD pattern attributed to the graphite (0 0 2) plane, which was also reflected in HRTEM images. It can be found that after hybridizing NMs with CDs, there was no considerable change in the crystal structure of each component [93]. In Song et al. report [91], the HRTEM of Ag@CDs NPs showed clear fringe spacing of CDs and a face-centered-cubic (fcc) polycrystalline structured Ag NPs (Fig. 2G). They found that in XRD patterns, the carbon characteristic peak of CDs at 25° was so weak that it could not be observed, and only characteristic peaks of Ag occurred (Fig. 2H). The additional peaks at 33.5° and 55.7° were attributed to the O = C-O-Ag due to the large number of carboxyl groups on the CDs.

#### 3.2. Microscopy characterization

Transmission electron microscopy (TEM) of NMs/CDs is usually employed to provide information about morphologies, particle sizes, properties of distribution and morphological parameters. In the system of surfactant-free Au NPs/reduced-CDs (sf-Au NPs/r-CDs), the morphology of Au NPs and CDs was characterized by TEM [68]. As displayed in Fig. 3A, the CDs with an average size of 3.5 nm and the sf-Au NPs/r-CDs with an average size of 15 nm were dispersed well, in which the lattice fringe of 0.235 nm could be ascribed to the spacing of the (1 1 1) planed in face-centered cubic Au NPs. Also, r-CDs were encompassed on the surface of Au NPs, confirming the morphology structure of the nanohybrids. In the case of Ag/N-GQDs/g-C<sub>3</sub>N<sub>4</sub> (AGCN-4) [52], the morphology of N-GQDs and Ag NPs could be clearly observed in the TEM and HRTEM images (Fig. 3B), indicating the co-existence N-GQDs and Ag NPs on g-C<sub>3</sub>N<sub>4</sub> nanosheet. It can be seen that Ag NPs and N-GQDs stuck together and firmly contacted with g-C<sub>3</sub>N<sub>4</sub>, indicating that during depositing Ag NPs on N-GQDs/g-C<sub>3</sub>N<sub>4</sub>, the electrons tended to transport and accumulate on the surface of N-GQDs and thereby reduced Ag<sup>+</sup> to form Ag.

#### 3.3. Optical and photochemical properties

To investigate the optical and photochemical properties of NMs/CDs, UV-visible-near-infrared (UV-vis-NIR) diffuse reflectance spectroscopy (DRS), transient photocurrent response, and electrochemical impedance spectroscopy (EIS) and photoluminescence (PL) spectra are routine characterization tools [91,94]. Single component NMs is not a semiconductor for photocatalytic processes, but NMs/CDs nanohybrids combined with other suitable semiconductors can serve as effective photocatalysts. From DRS reflectance spectrum comparison between different composite samples g-C<sub>3</sub>N<sub>4</sub>, N-GQDs/g-C<sub>3</sub>N<sub>4</sub> (GCN-3), and Ag/g-C<sub>3</sub>N<sub>4</sub>, and Ag/N-GQDs/g-C<sub>3</sub>N<sub>4</sub> (AGCN-4) (Fig. 3C), AGCN-4 exhibited higher light absorption ability than others from visible light region to NIR light region [52]. The emerging peaks in the range of 450–550 nm could be ascribed to the LSPR effect of Ag NPs. In addition, transient photocurrent response and EIS were employed to study the charge transfer and separation of NMs/CDs [41,52,74,95]. As displayed in Fig. 3D and E, AGCN-4 exhibited highest photocurrent density in both visible light region and NIR light region, and presented best electronic conductivity, in which the smaller diameter indicates the weaker impedance and more efficient charge transfer. These results indicated that the synergistic effect of N-GQDs and Ag NPs could effectively separate the photogenerated electron-hole pairs. From the PL spectra in Fig. 3F, the AGCN-4 displayed lowest PL intensity, illustrating that the recombination process of the charges was effectively suppressed.

### 4. Environment-Related applications

The broad range of chemical pollutants produced in production and daily life including heavy metals and organic pollutants et al., have threaten the environmental security and human health [96]. The efficient degradation and detection of various toxic chemical pollutants are important for preventing and controlling the pollutants [97]. Each NMs/CDs in different application has its own characteristic depending on the applied conditions. For example, the fluorescence resonance energy transfer (FRET) from CDs to NMs was utilized to construct a ratiometric fluorescent sensor for pollutants detection, while in photocatalytic application, the FRET occurred when the distance between CDs and NMs was too close, adversely quenching the photogenerated charge carriers [10].

In this section, firstly, the recent applications of NMs/CDs hybrids in catalytic reduction and photocatalytic degradation and its characteristic in different applied conditions were reviewed. Then, various NMs/CDs nanohybrids for the construction of sensors/biosensors were summarized in some recent studies. Catalytic reduction using NMs/CDs involves hydrogenation reactions, such as hydrodeoxygenation, hydrodehalogenation and hydrogenolysis, in which pollutants are reduced to less toxic and more readily biodegradable products, rather than directly mineralized into CO<sub>2</sub> and H<sub>2</sub>O [98,99]. While in photocatalytic degradation of pollutants, NMs/CDs are excited by light irradiation to produce electron-hole pairs, in which electrons in conduction band react with O<sub>2</sub> to produce superoxide radical, and holes with strong oxidation ability directly react with pollutants or H<sub>2</sub>O to produce hydroxyl radical, which can both mineralize pollutants [100].

#### 4.1. Catalytic reduction

The catalytic reduction in treating water has been extensively studied in the laboratory, and its applications also demonstrated satisfying results on actual wastewater, which could yield products with substantially less toxic and more readily biodegradable products [7]. For instance, NMs/CDs composites have been employed in the simple reduction of nitro aromatic compounds to the corresponding amino aromatic compounds by using NaBH<sub>4</sub> as reductant, which can reduce the toxicity of pollutants and is a convenient method to convert organics to value added intermediates [62,72,90,101]. In these NMs/CDs



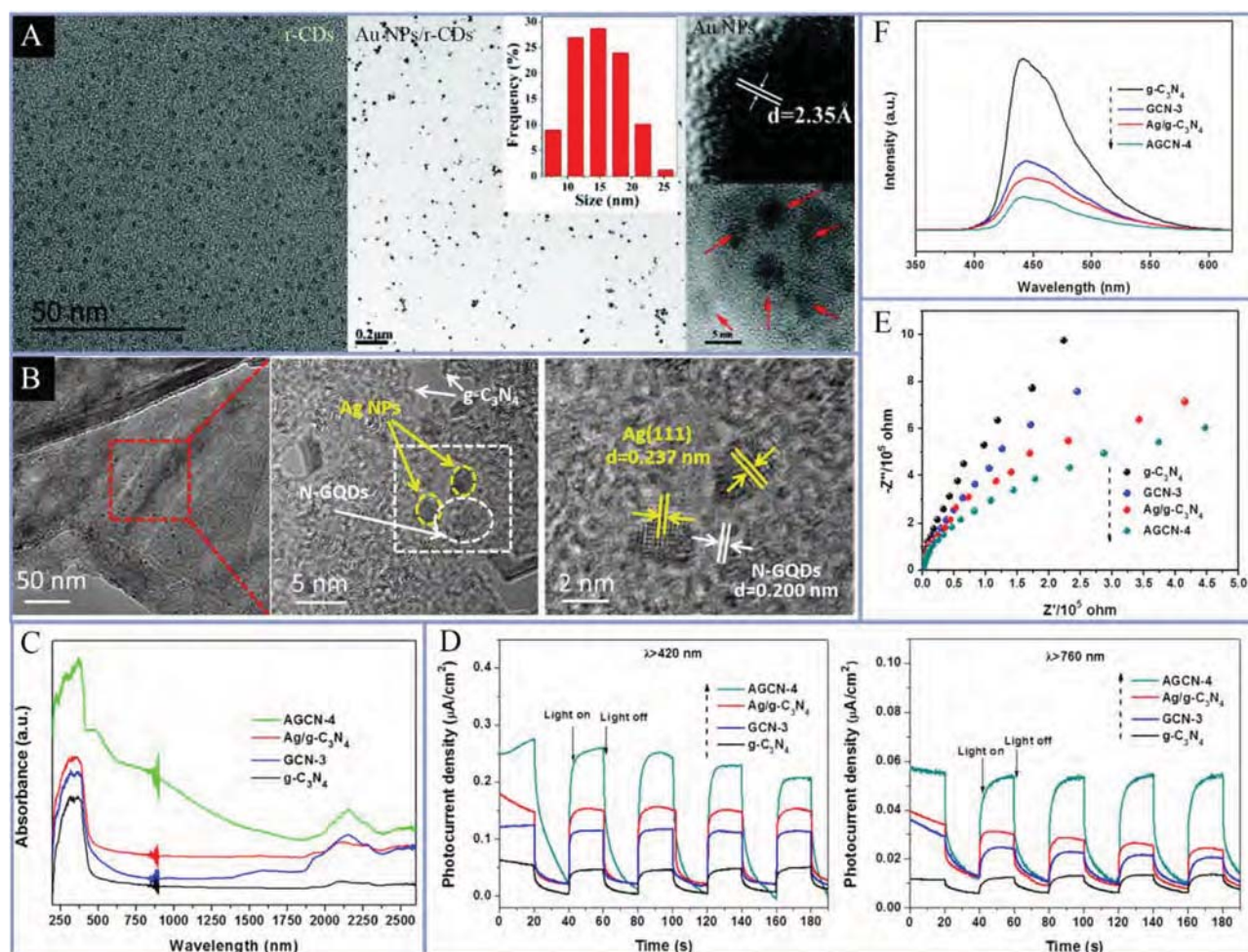


**Fig. 3.** (A) TEM images of r-CDs, size distribution of the synthesized sf-AuNPs/r-CDs and HRTEM images of sf-AuNPs/r-CDs. Reprinted from Ref. [65] with permission from The Royal Society of Chemistry. (B) TEM and HRTEM images of AGCN-4. (C) UV-vis-NIR diffuse reflectance spectra, (D) Transient photocurrent responses, and (E) EIS Nyquist plots, and (F) PL spectra of g-C<sub>3</sub>N<sub>4</sub>, GCN-3, and Ag/g-C<sub>3</sub>N<sub>4</sub>, and AGCN-4. Reprinted from Ref. [49] with permission from American Chemical Society.

composites for nitro aromatic compounds reduction, NMs are main catalytic active centers and CDs behave as stabilizers or enhancers for NMs to promote electron transfer, representing a simple synergy between NMs and CDs. In detail, the synergistic effect of CDs and NMs plays a significant role on the enhanced catalytic activity in these reduction reactions: (i) The surface groups of CDs guarantee the dispersivity and stability of NMs with large number of exposed metal atoms, exhibiting high catalytic activity, (ii) The abundant surface groups of CDs adsorb more reactants and thereby facilitate catalytic reaction [75,101], and (iii) The good electronic properties of NMs and CDs can boost the electron transfer for catalytic reactions.

For instance, Zheng et al. synthesized surfactant-free Au NPs/r-CDs composites for 4-nitrophenol (4-NP) reduction. The Au NPs with surfactant-free property exhibited high catalytic activity and r-CDs with excellent electronic properties greatly accelerated the electron transfer, improving the catalytic activity [68]. Recently, an immobilized (Au/GQDs)<sub>10</sub> multilayer thin film on fluorine-doped tin oxide substrates was synthesized by Xiao et al., which exhibited remarkable catalytic performance in the 4-NP reduction and were significant for practical applications since no separation of catalyst is needed [39]. As shown in Fig. 4A-C, a characteristic peak at 400 nm ascribed to 4-NP weakened by degrees, while the peak at 300 nm ascribed to 4-AP increased correspondingly, indicating the reduction of 4-NP. The catalytic activity of (Au/GQDs)<sub>10</sub> films was almost 4 and 12 times higher than that of Au NP s and (GQDs)<sub>10</sub> counterpart films, respectively (Fig. 4D-F). To reveal the

high catalytic activity, they probed the electronic properties of (Au/GQDs)<sub>10</sub> films by conductive atomic force microscopy (c-AFM) in the applied imaging mode, and the dark current measurements (Fig. 4G and H) exhibited an image-average current of 171.3 pA for the (Au/GQDs)<sub>10</sub> films, which was over 30 times higher than that of the (Au)<sub>10</sub> films of 5.6 pA. The high average current of (Au/GQDs)<sub>10</sub> was revealed by the bright area (high-current) among the whole scanned area. This observation implied a continuous electron transfer network in (Au/GQDs)<sub>10</sub> films, thereby resulting in effective electron transfer, remarkable current density and boosted catalytic activity. Hence, the enhanced catalytic performance of (Au/GQDs)<sub>10</sub> films were ascribed to the efficient electron transfer between GQDs and Au NPs. Besides, the integrative roles of GQDs in preventing the Au NPs aggregation could guarantee the activity of Au NPs [70]. In addition, the zero-dimension GQDs possessed abundant active sites in the zigzag edges of GQDs, which interplayed with the terminal O atoms of 4-NP and thus efficiently weakened the N – O bonds, thus triggering 4-NP reduction reactions (Fig. 4I). Recently, a thermos-sensitive copolymers (catechol-terminated thermo-responsive copolymer) functionalized Fe<sub>3</sub>O<sub>4</sub> supported CDs@Pd NPs were constructed for effective catalytic reduction [102]. The high catalytic efficiency was ascribed to the accelerated electron transfer and well-dispersed Pd NPs caused by CDs. Additionally, the modified hydrophilic polymer could help immobilize Pd NPs to guarantee the active sites [89].

NMs/heteroatoms doped CDs composites are also developed to

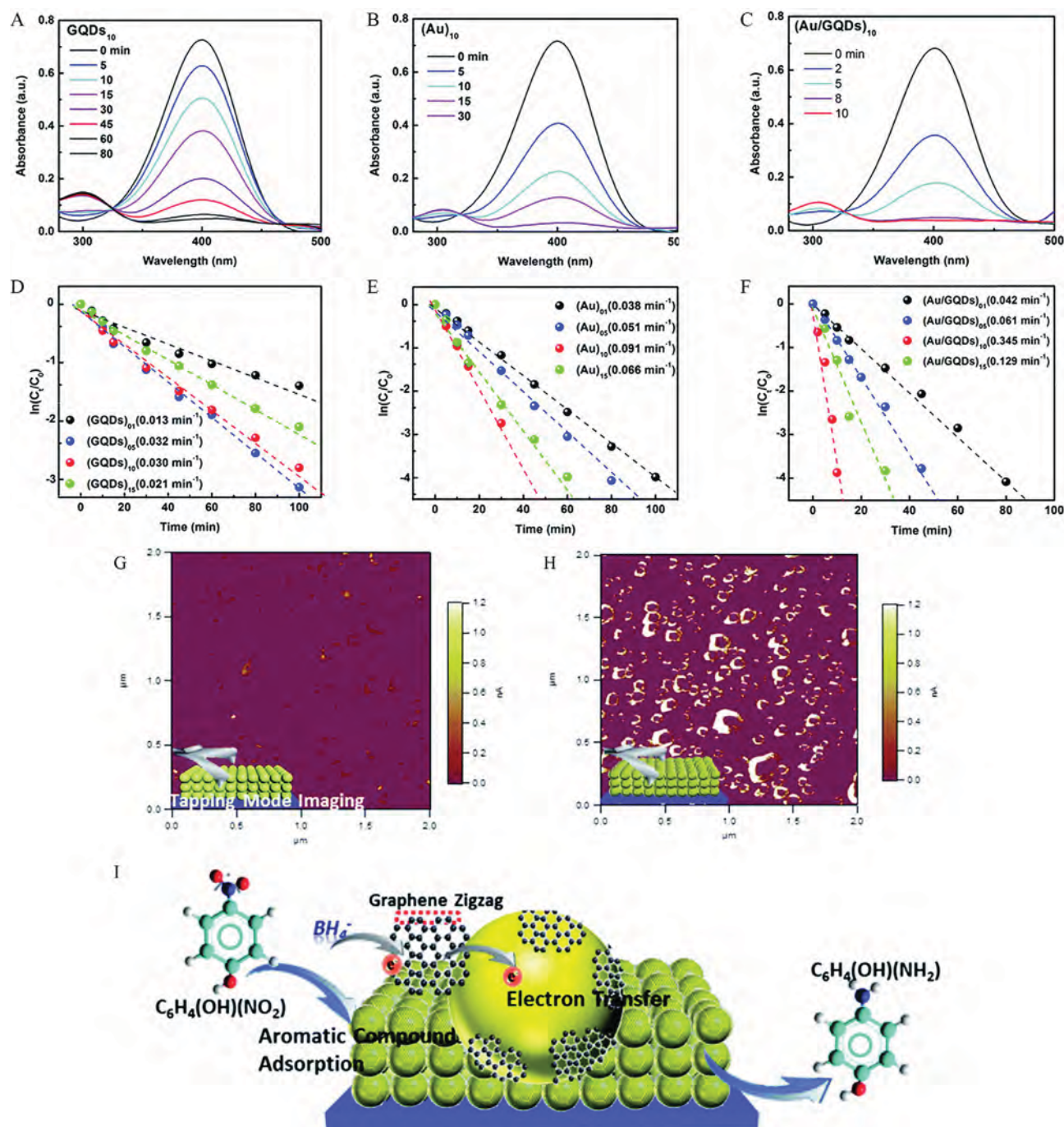


**Fig. 4.** Time-dependent UV-Vis absorption spectra of 4-NP reduction over the (A)  $\text{GQDs}_{10}$ , (B)  $(\text{Au})_{10}$ , and (C)  $(\text{Au/GQDs})_{10}$  films. Plots of  $\ln(C_t/C_0)$  versus reaction time for the reduction of 4-NP over the (D)  $\text{GQDs}_{10}$ , (E)  $(\text{Au})_{10}$ , and (F)  $(\text{Au/GQDs})_{10}$  films. c-AFM dark current images of (G)  $(\text{Au})_{10}$  films and (H)  $(\text{Au/GQDs})_{10}$  films with 10 mV bias potential. (I) The catalytic mechanism of  $(\text{Au/GQDs})_{10}$  films for 4-NP degradation. Reprinted from Ref. [39] with permission from The Royal Society of Chemistry.

attune the catalytic property. The heteroatoms doped in CDs further enhance the interaction between CDs and NMs. Chen et al. synthesized Au NPs on GQDs doped with N atoms [103]. The XPS spectra showed that compared to the XPS peak of  $\text{Au}^0$  at 87.4 eV, the peak of  $\text{Au}^0$  in Au NPs-NGQDs shifted to 87.8 eV, ascribed to the interaction between Au and N atoms. It illustrates that the doped N atoms provided abundant active sites for Au NPs anchoring and made Au NPs well disperse, thereby guaranteeing the reusability and producing high catalytic activity with rate constant of  $1.17 \times 10^{-2} \text{ s}^{-1}$ . Amita et al. synthesized N, S doped CDs-Au NCs composites, which exhibited excellent activity with rate constant of  $1.37 \times 10^{-1} \text{ s}^{-1}$  [93]. The superior catalytic

activity was ascribed to the well-dispersed Au NPs on N, S co-doped CDs and the accelerated electron transfer in the catalytic system.

Except the Au and Ag, a representative example indicated the importance of electron transfer and interaction strength between the NMs and CDs was reported in the Pd@N, S-CQDs materials by Lu and his coworkers [104]. They investigated the catalytic activity and selectivity of N, S-CQDs-Pd in hydrogenation of p-chloronitrobenzene (p-CNB), and the surface interaction among N, S-CQDs and Pd. Under the catalysis of Pd NPs, N, S-CQDs specially targeted Pd particles due to the surface reactions between C-S/C-N groups of N, S-CQDs and C-O groups of carbon matrix. The C-N groups of N, S-CQDs fixed N, S-CQDs on



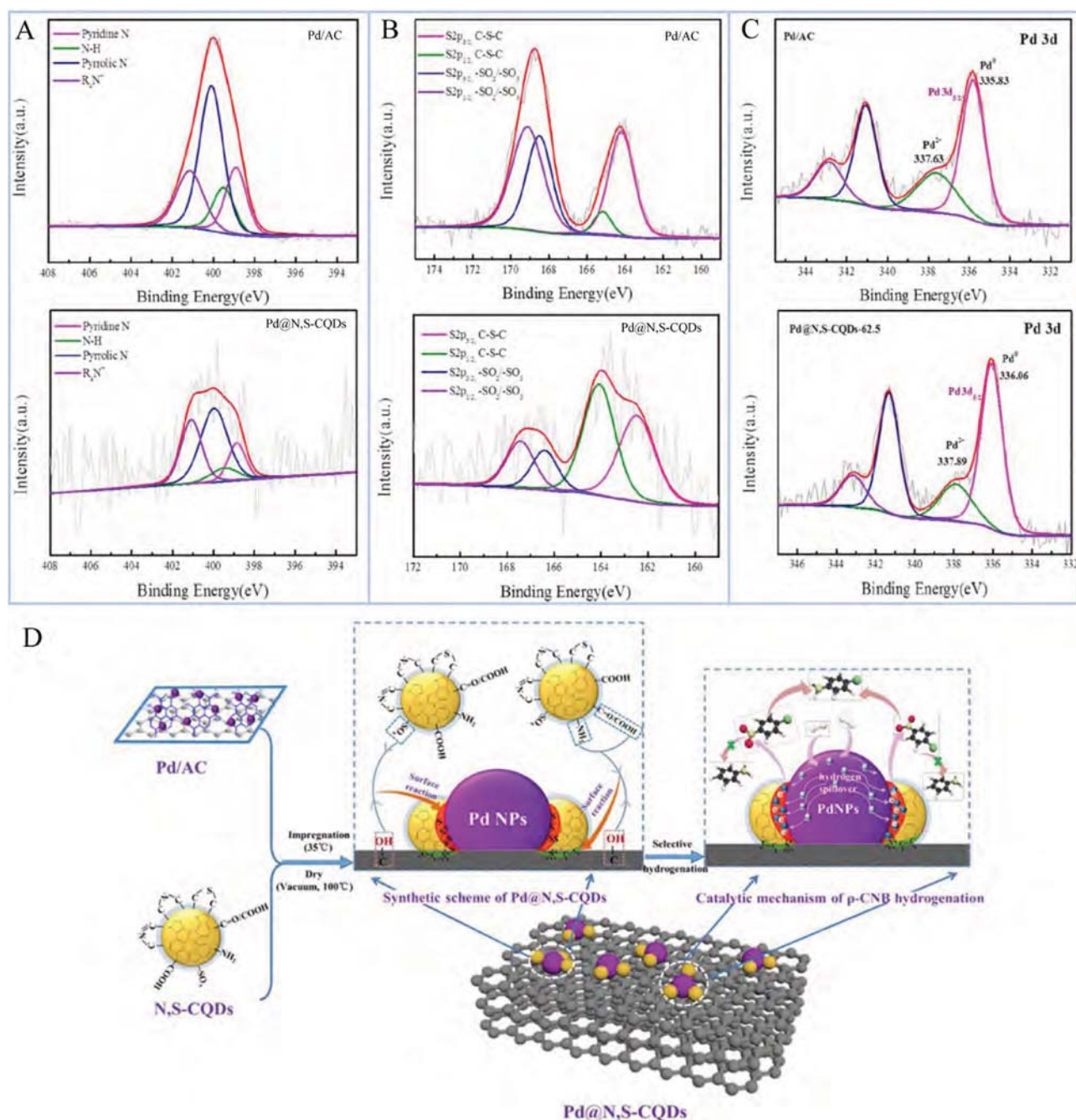


**Fig. 5.** (A) XPS spectra of N 1s, (B) XPS spectra of S 2p, and (C) XPS spectra of Pd 3d of Pd/AC and N,S-CQDs. (D) The catalytic mechanism of Pd@N,S-CQDs for halonitrobenzene hydrogenation. Reprinted from Ref. [104] with permission from American Chemical Society.

carbon support, and the transformation of S-containing groups of N, S-CQDs into C-S-C over the Pd particles contributed a strong interaction between Pd and S, thereby making strong interaction between Pd, N, S-CQDs and carbon matrix. It would guarantee excellent structure stability of Pd@N, S-CQDs. In addition, they found binding energies (BE) of N-containing groups maintained no changed between N,S-CQDs and Pd@N, S-CQDs (Fig. 5A), while BE of S-containing groups of Pd@N, S-CQDs displayed significant negative shift (Fig. 5B) and BE of Pd<sup>0</sup> had positive shift (Fig. 5C). It verified the electrons transferred from Pd to S groups while no electrons transferred between Pd and N. In hydrogenation of halonitrobenzene, electrons on Pd transferring to S played a part as a reservoir and gathered most dissociated hydrogen due to the hydrogen spillover (Fig. 5D). The dissociated hydrogen with negative charge due to the electron rich properties of S groups, resulted in a

superior conversion and selectivity of Pd@N,S-CQDs for hydrogenation of halonitrobenzene. In addition to monometallic NPs/CDs composites, bimetallic NPs/CDs were also developed for the catalytic reduction of 4-NP [65,105,106]. For instance, Au<sub>x</sub>Ag<sub>y</sub>@C-dots with a size range of 1.9–3.4 nm were synthesized by Baker et al [105]. Compared with monometallic Au or Ag/CDs composites, the catalytic activity was significantly enhanced. Moreover, the catalyst displayed an excellent stability and completely preserved the apparent rate constants for 4-NP reduction, owing to the minor NMs aggregation.

#### 4.2. Photocatalytic degradation of pollutants

Photocatalytic degradation of pollutant is an important and extensive issue of concern to the scientific community [107–109]. On

account of its high efficiency and low energy consumption, photocatalysis has been demonstrated to be a promising environmental purification technology [110–112]. NMs possess unique electronic properties and strong absorption of visible light owing to SPR effect [3,22,91]. CDs with unique electronic and light-absorbing properties are a promising alternative to semiconductor QDs and molecular dyes in photocatalytic applications [43,113]. Hence, many heterojunction photocatalytic materials composed of NMs and CDs have been developed [41,52]. In the above discussion of synergistic effect between NMs and CDs in catalytic reduction, the catalytic activity almost comes from NMs, and CDs rarely exhibits their catalytic behavior. For photocatalytic degradation, the catalytic activity can come from both NMs and CDs. They both can function as catalytic center, providing a platform for excited electrons to reduce  $O_2$  to produce  $\cdot O_2^-$  and even serving as an electron bridge for better charge carriers separation. In general, NMs integrated with CDs can accomplish the following tasks: (i) promoting charge separation via heterojunctions, (ii) exciting electrons to a higher state and mediate electron transfer by SPR effect, and (iii) up-converting long wavelengths to shorter wavelengths, thereby expanding the light utilization.

Among NMs, Au and Ag stand for the most investigated metals exhibiting LSPR effect in visible region, which were integrated with CDs for photocatalytic applications. For example, Li et al. synthesized a ternary photocatalyst Ag-GQDs-ZnO for Rhodamine B (RhB) degradation under visible light irradiation [74]. After 8 h reaction, the removal efficiency of RhB for pristine ZnO film, GQDs-ZnO film, Ag-ZnO film, and Ag-GQDs-ZnO film was 23.43%, 32.30%, 48.59%, and 57.49%, respectively. The enhanced RhB degradation efficiency of Ag-GQDs-ZnO film was attributed to the synergistic effect between Ag NPs and GQDs (Fig. 6A). To further improve the degradation efficiency of RhB and study the role of Ag NPs and GQDs, the same research group later synthesized GQDs-Ag composites by using GQDs as reduction agent and found that 4  $\mu\text{g/mL}$  of RhB was degraded completely by GQDs-Ag in 9 h [19]. In these catalytic system, SPR effect of Ag NPs was exploited to

excite electrons below the Fermi level to surface plasmon states by visible light irradiation. GQDs would impede charge-carriers recombination and serve as electron sink, in which the trapped electrons continued to reduce  $O_2$  to produce  $\cdot O_2^-$ .

In some cases, benefiting from the superior electronic properties, high ability of light absorption and low recombination rate of charge-carriers, NMs and CDs were used to construct multi-steps charge transfer channel in full-spectrum, which could greatly improve the photocatalytic efficiency of pollutants degradation. In a study, ternary plasmonic CQDs/Ag/Ag<sub>2</sub>O was synthesized by a homogeneous precipitation method, which was carried out for photocatalytic degradation of MB under UV, visible and NIR light irradiation [41]. As show in Fig. 6B and C, Ag/Ag<sub>2</sub>O exhibited a broader background absorption compared to Ag<sub>2</sub>O, demonstrating the SPR effect of Ag NPs facilitated the light absorption. And CQDs/Ag<sub>2</sub>O and CQDs/Ag/Ag<sub>2</sub>O displayed strong absorption in the light range of 250–2500 nm compared to Ag/Ag<sub>2</sub>O, indicating that CQDs can adsorb NIR light and then convert it to a shorter wavelength light. The results showed degradation efficiency of MB over CQDs (30 mL)/Ag (0.40 wt%)/Ag<sub>2</sub>O under UV light irradiation was 95% within 80 min, and under visible light irradiation almost 100% within 120 min, which were higher to the Ag<sub>2</sub>O, Ag/Ag<sub>2</sub>O and CQDs/Ag<sub>2</sub>O counterparts (Fig. 6D). Additionally, the photocatalytic performance of CQDs (30 mL)/Ag (0.40 wt%)/Ag<sub>2</sub>O displayed the most excellent catalytic activity among all the catalysts under 150 min NIR light irradiation, indicating the ternary CQDs (30 mL)/Ag (0.40 wt%)/Ag<sub>2</sub>O exhibit excellent catalytic activity in full-spectrum. The accelerated catalytic activity is due to the superior light absorption efficiency of CQDs/Ag/Ag<sub>2</sub>O, originated from the SPR effect of Ag NPs and up-conversion property of CQDs, which were demonstrated by the optical absorption spectra and UV-vis-NIR DRS. Benefiting from the electron bridge of CQDs, the efficient multi-steps electrons transfer channel Ag<sub>2</sub>O → CQDs → Ag was constructed, in which the holes on Ag<sub>2</sub>O could directly react with pollutant, and electrons would further transfer to CQDs and Ag, then reducing  $O_2$  to  $\cdot O_2^-$  (Fig. 6E). Similarly,

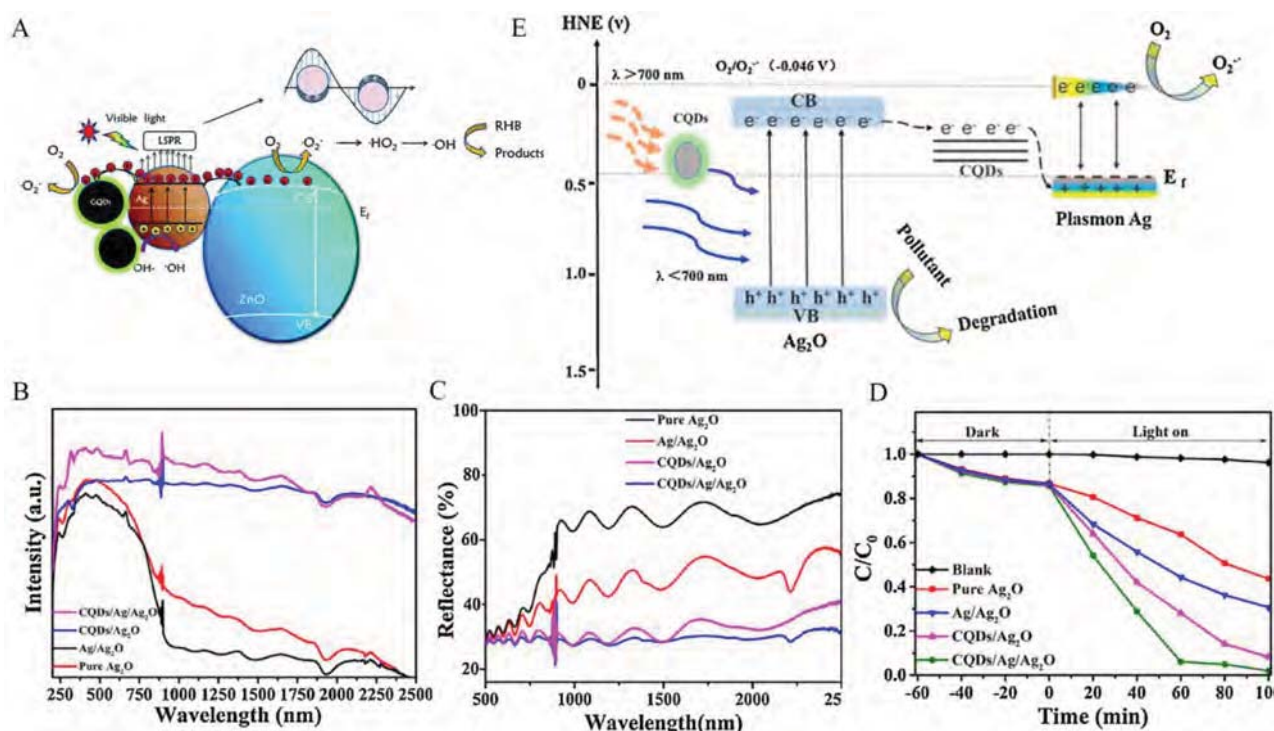


Fig. 6. (A) The catalytic mechanism of Ag-GQDs-ZnO ternary composite film for RhB degradation. Reprinted from Ref. [74] with permission from Royal Society of Chemistry. (B) Optical absorption spectroscopy and (C) UV-Vis-NIR DRS reflectance spectra of Ag<sub>2</sub>O, Ag/Ag<sub>2</sub>O, CQDs/Ag<sub>2</sub>O and CQDs/Ag/Ag<sub>2</sub>O. (D) The degradation efficiency of MB by Ag<sub>2</sub>O, Ag/Ag<sub>2</sub>O, CQDs/Ag<sub>2</sub>O and CQDs/Ag/Ag<sub>2</sub>O composites under UV irradiation. (E) The degradation mechanism of MB by CQDs/Ag/Ag<sub>2</sub>O. Reprinted from Ref. [41] with permission from Elsevier.

**Table 2**  
The catalytic reduction and photocatalytic degradation applications of NMs/CDs hybrids.

Hybrids	Catalytic system	Pollutants	Catalytic activity (rate constant of efficiency)	Experimental condition	Ref.
Au NPs/r-CDs	Catalytic reduction	4-NP	0.75 min <sup>-1</sup>	NaBH <sub>4</sub> as reductant	[68]
Fe <sub>3</sub> O <sub>4</sub> @C-dot/Ag NCs	Catalytic reduction	p-nitroaniline (4-NA)	1.5478 min <sup>-1</sup>	NaBH <sub>4</sub> as reductant	[62]
Au@CD@P <sup>a</sup>	Catalytic reduction	2-nitrophenol (2-NP); 3-nitrophenol (3-NP); 4-NP	0.176 min <sup>-1</sup> ; 0.761 min <sup>-1</sup> ; 0.602 min <sup>-1</sup>	NaBH <sub>4</sub> as reductant	[90]
CDs/Ag@Mg-Al-Ce-LDH <sup>b</sup>	Catalytic reduction	4-NP; Congo red (CR); Rhodamine 6G (R6G); Methylene blue (MB); Methyl orange (MO)	2.28 min <sup>-1</sup> ; 1.44 min <sup>-1</sup> ; 3.3 min <sup>-1</sup> ; 1.38 min <sup>-1</sup>	NaBH <sub>4</sub> as reductant	[70]
Pd@N,S-CQDs	Catalytic reduction	p-CNB	1.92 min <sup>-1</sup>	NaBH <sub>4</sub> as reductant	[104]
CDs/Ag/P25 <sup>c</sup>	Photocatalytic degradation	MB	100% degradation within 15 min	8 W UV lamp	[84]
P <sub>AAr</sub> -CQD/TiO <sub>2</sub> <sup>d</sup>	Photocatalytic degradation	MB; Erythromycin	~96% degradation within 20 min; ~92% degradation within 150 min;	250 W UV lamp	[168]
CQDs/Ag/Ag <sub>2</sub> O	Photocatalytic degradation	MB	100% degradation within 120 min;	250 W Xe lamp with 420 nm cutoff filter	[41]
Fe/Ag@CQDs BMNCs <sup>e</sup>	Photocatalytic degradation	Fast green (FG)	74% degradation within 60 min	500 W Xe lamp with 420 nm cutoff filter	[169]
SDAg-CQDs/UCN	Photocatalytic degradation	Naproxen	87.5% degradation within 25 min	350 W Xe lamp with 420 nm cutoff filter	[114]

<sup>a</sup> P, poly(N-isopropylacrylamide). <sup>b</sup> Mg-Al-Ce-LDH, magnesium–aluminum layered double hydroxide. <sup>c</sup> P25, TiO<sub>2</sub> (commercial Degussa P25). <sup>d</sup> P<sub>AAr</sub>, plasmonic Au nanostructures. <sup>e</sup> BMNCs, bimetallic nanocomposite.

Ag NPs and N-GQDs co-modified g-C<sub>3</sub>N<sub>4</sub> was synthesized by Tang et al [52], which presented a 90.11% of tetracycline degradation efficiency in 60 min. The high photocatalytic activity of Ag (2.0 wt%)/N-GQDs (0.5 wt%)/g-C<sub>3</sub>N<sub>4</sub> for antibiotic tetracycline degradation was due to the synergistic effect of Ag NPs, GQDs and g-C<sub>3</sub>N<sub>4</sub>, which could enhance light absorption and accelerate charge carrier migration [84]. Further, a single atom-dispersed Ag and CQDs co-loaded ultrathin g-C<sub>3</sub>N<sub>4</sub> (SDAg-CQDs/UCN) was developed, which showed excellent catalytic activity with a 87.5% degradation of naproxen (NPX) in 25 min [114].

The comparison of NMs/CDs performance in catalytic reduction and photocatalytic degradation of pollutants is listed in Table 2. In brief, the catalytic reduction with NMs/CDs nanohybrids applies to dyes and refractory organic pollutants with toxic groups such as –NO<sub>2</sub>, –N = N–, and halogenated group (–Cl, –Br), which can decolorize the color of dyes and convert the high toxicity of pollutants to low toxicity in the presence of reductant such as NaBH<sub>4</sub>. Considering it exhibits high catalytic efficiency, the catalytic reduction with NMs/CDs applies to preliminarily treat wastewater. However, the mineralization rate in the catalytic reduction is relatively low, which often needs advanced treatment to mineralize pollutants. In contrast, the photocatalytic degradation exhibits relatively low photocatalytic efficiency. But it has high mineralization rate, and the produced radicals during photocatalytic reaction have no selection on pollutants. Hence, the photocatalytic degradation with NMs/CDs has extensive adaptability and applies to treat kinds of refractory organic pollutants. However, the photocatalytic degradation needs light irradiation, resulting that it is not suitable for treating the dyeing wastewater with color depth. Overall, a comparative ideal method for the pollutants removal in wastewater is to combine the catalytic reduction and photocatalytic degradation. Specifically, the catalytic reduction is firstly used to decolorize the dyes and then photocatalytic degradation is used for further advanced treatment to improve the mineralization rate of pollutants [115,116].

#### 4.3. Detection of environmental pollutants

It has been widely reported that the applications of NMs/CDs nanohybrids in detection are highly sensitive and rapid response [69,117]. In this section, we mainly focus on the various NMs/CDs nanohybrids for the construction of sensors/biosensors by employing some typical examples. The comparison of NMs/CDs hybrids on various targets in different detection systems are listed in Table 3.

##### 4.3.1. Fluorescent detection

In recent years, CDs and NMs (especially Au and Ag NPs) have come to the fore as two new class of fluorescent nanomaterials due to their particular fluorescence properties and stability [87]. Hence, NMs/CDs nanohybrids are generally chosen as metal ion sensors to determine the ion concentration by fluorescence detection [63,66]. Among them, CDs serve as fluorescence reporter because it is efficient energy donors, thereby realizing pollutant detection by color change [63]. Moreover, the design routes are based on the interaction effect between fluorescence property of CDs and plasmonic activity of single NMs, namely, the NMs could induce the fluorescence enhancement of the CDs, realizing a typical metal-enhanced fluorescence (MEF) technology [20,118]. It was shown in an study reported by Ma et al. with a fluorescence enhanced sensing method for detecting heavy metal-copper ions (Cu<sup>2+</sup>) [119]. In their study, the sensing system containing propiolic acid-tagged CDs and 4-azidobenzoic acid-tagged Au@SiO<sub>2</sub> was utilized to measure Cu<sup>2+</sup> by the reducing Cu<sup>2+</sup> into Cu<sup>+</sup>. And as the Cu<sup>+</sup> concentration increased, the fluorescence signal was continuously enhanced (released by CDs and further magnified by Au core via commanding the distance between CDs and Au NPs), thereby realizing the high-efficient detection.

Furthermore, the “dual-emission” ratiometric fluorescent sensors were constructed [81]. For instance, Shan et al. [88] established an



**Table 3**

The detection performance of NMs/CDs hybrids on various targets in different detection systems.

Detection systems	Hybrids	Targets	Detection limit	Linear response range	Ref.
Fluorescent detection	CQDs/Au NCs	$\text{Cd}^{2+}$	32.5 nM	0.15 to 15 mM	[88]
	C-Au NCs modified with DTT	$\text{Hg}^{2+}$	8.7 nM	50 to 1000 nM	[120]
	Au NCs-CDs	$\text{Hg}^{2+}$ ; $\text{Cr}^{6+}$	1.85 nM; 5.34 nM	1 to 100 nM; 50 to 10 $\mu\text{M}$	[121]
	Au NPs/CQDs	Organophosphorus pesticides	0.18 nM	0.18 to 180 nM	[125]
	Au NPs/N, P-doped carbon quantum dots	Carbendazim	0.002 $\mu\text{M}$	0.005 to 0.16 $\mu\text{M}$	[126]
	N-CQDs/AuNCs	Carbendazim	0.83 $\mu\text{M}$ ; 37.25 $\mu\text{M}$	1–100 $\mu\text{M}$ ; 150–1000 $\mu\text{M}$	[170]
Colorimetric detection	CDs-Ag NPs	$\text{Cu}^{2+}$	0.037 $\mu\text{M}$	0.3 to 8 $\mu\text{M}$	[61]
	Au@g-CNQDs	$\text{Cd}^{2+}$	10 nM	0.01–3.0 $\mu\text{M}$	[171]
	Ag/CQDs	$\text{Hg}^{2+}$	85 nM	0.5 to 50 $\mu\text{M}$	[73]
	AuNP/CDs	$\text{Hg}^{2+}$	7.5 nM	10 to 300 nM	[128]
Electrochemical detection	Au NPs@NCDS@Ag NPs	Metobromuron	0.0002 nM	0.001 to 2 nM	[92]
	Ag@CQDs	$\text{Cl}^-$	0.33 nM	0.99 to 450 nM	[135]
	Ag-C-dot	$\text{S}^{2-}$	0.027 $\mu\text{M}$	0.05 to 100 $\mu\text{M}$	[136]
Electrochemilumin-escence detection	Pd@Au HOHs/N-CDs	$\text{Pb}^{2+}$	0.33 ng/mL	1.0 to 1375.0 ng/mL	[139]

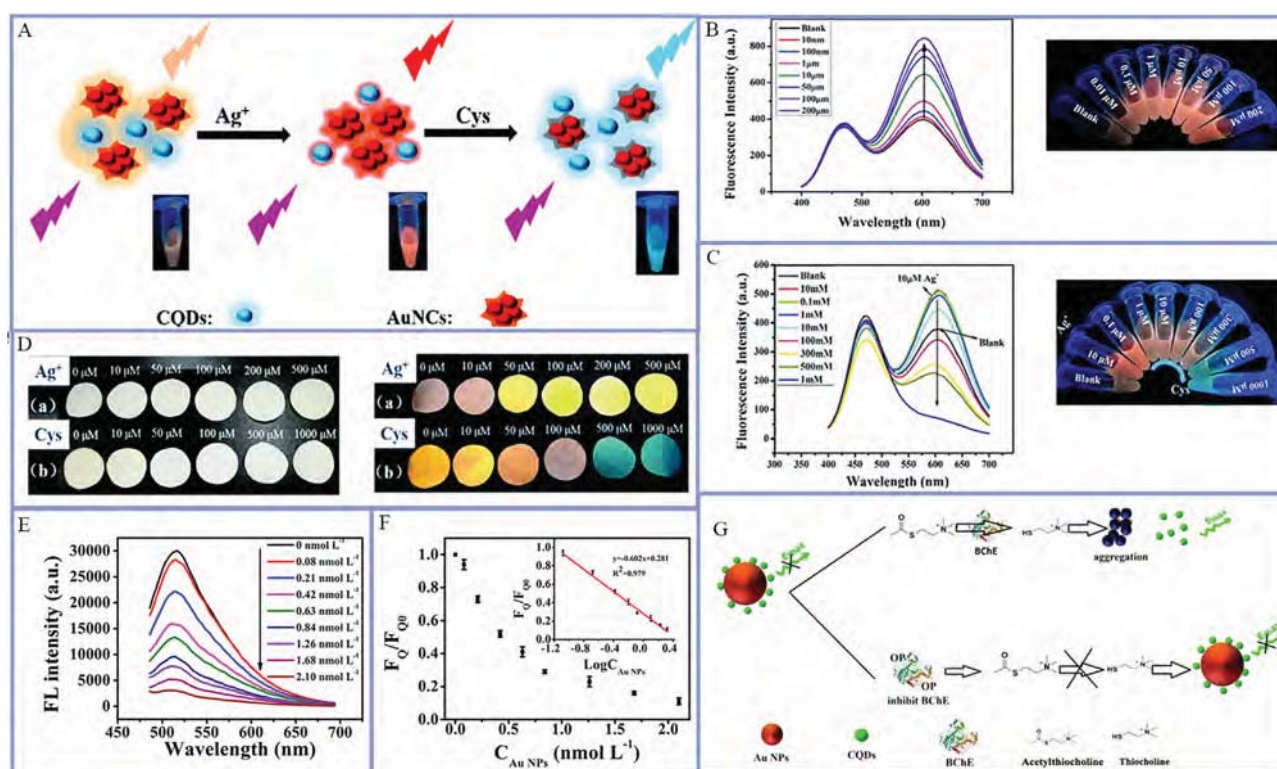


**Fig. 7.** (A) Schematic illustration of the dual-emission system of CQDs and Au NCs. Fluorescence spectra of the system (B) in the presence of  $\text{Ag}^+$  and (C) in the presence of  $\text{Ag}^+$  and different concentrations of Cys. (D) The photographs of the paper sensors under daylight (left) and a 365 nm UV lamp (right). Reprinted from Ref. [87] with permission from Royal Society of Chemistry. (E) The fluorescence spectra of CQDs in presence of Au NPs. (F) The quenching percentages ( $F_0/F_{00}$ ) by the different Au NPs concentrations. Inset: the linear relationship with Au NPs logarithmic concentration. (G) The mechanism of FRET-based sensing system for OPs detection. Reprinted from Ref. [125] with permission from Elsevier.

efficient CQDs/Au NCs nanohybrid as a ratiometric fluorescent probe for cadmium ions ( $\text{Cd}^{2+}$ ) and AA detection. Upon the additional of  $\text{Cd}^{2+}$ , the cubic aggregation would be formed owing to electrostatic and metal–ligand coordination. This would result in the fluorescence quenching of Au NCs. However, the fluorescence of CQDs almost remained unchanged, thereby achieving a ratiometric strategy for detecting  $\text{Cd}^{2+}$ . Similarly, Kang et al. reported a dual-emission CDs-Au nanoclusters (C-Au NCs) functionalized with dithiothreitol (DTT) for detecting  $\text{Hg}^{2+}$  [120]. Owing to the robust metallophilic interaction between  $\text{Hg}^{2+}$  and  $\text{Au}^+$ , most  $\text{Hg}^{2+}$  could be interacted to C-Au NCs surface modified with DTT. Then, the orange-red fluorescence ascribed to Au NCs emission was quenched, while blue fluorescence ascribed to CQDs emission was almost invariably to achieve the detection of  $\text{Hg}^{2+}$ . The detection system showed a lower detection limit of 8.7 nM and a

wide linear range of 50–1000 nM. Furthermore, the CQD/Au NC nanohybrids as a dual-signal ratiometric fluorescent sensor were developed for  $\text{Ag}^+$  and L-cysteine (Cys) detection, which was reported by He et al. (Fig. 7A) [87].  $\text{Ag}^+$  would enhance the orange fluorescence of Au NCs, but Cys could completely quench the fluorescence of Au NCs owing to the high affinity of coordination interaction for Cys and  $\text{Ag}^+$ . On the contrary, the blue fluorescence of CQDs was not affected and changed (Fig. 7B and C), which could be distinctly recognized by the naked eye, thus realizing a paper-based visual detection (Fig. 7D). These works used dual-emission in detection, which surpassed the single-emission probe. The ratiometric fluorescent sensors could provide more distinct color change under UV light and accurate measurement without the interference from complicated environment [87,121]. It was attributed to their built-in correction by comparison of

two emission intensity ratios between CDs and NMs (one fluorophore as a signal probe and the other as the reference), instead of using absolute intensity from a single emission intensity [122,123].

In addition, the coupling of NMs with CDs could lead to the quenching of CDs fluorescence due to FRET from CDs to NMs in ratiometric fluorescent sensors. The FRET-based sensing system generally consists of a fluorophore probe and a nano quencher that function as the acceptor–donor pair. The emission spectrum of a donor overlap with the absorption spectra of an acceptor may give rise to FRET [124]. Du and co-workers developed an FRET-based sensor for detecting organophosphate pesticides (OPs), which comprised of tunable fluorescence emission CQDs (donor) and Au NPs (acceptor), respectively [125]. The fluorescence of CQDs was effectively quenched by Au NPs via FRET (Fig. 7E and F), owing to the complementary overlap between the emission spectrum of CQDs and absorption spectrum of Au NPs, as well as the electrostatic interaction between electronegative Au NPs and electropositive CQDs. After additional of acetylthiocholine (ATC) and butyrylcholinesterase (BChE) into the sensing system, the thiocholine was generated from ATC catalyzed by BChE, resulting in aggregation of Au NPs and corresponding recovery of CQDs fluorescence emission. For OPs detecting, OPs would irreversibly restrain the catalytic activity of BChE, which would not result in the Au NPs aggregation. Thereby, the recovery efficiency of fluorescence emission of CQDs was reduced, realizing the detection of OPs (Fig. 7G). Subsequently, to enhance the fluorescence emission, a substantial improvement in the quantum yield was later realized by replacing the CQDs with N, P-doped CQDs. Ma et al. employed the FRET sensing system based on N, P-doped CQDs and Au NPs for detecting toxic carbendazim (methyl-1H-benzo[d]imidazol-2-ylcarbamate) [126]. As a result of FRET, the fluorescence of the N, P-CQDs was obviously quenched by Au NPs. In this sensing system, CQDs doping with heteroatoms N and P enhanced the quantum yield by modulating the band gap and electron density of CQDs, and improved the sensing performance [127].

In addition to FRET, nanometal surface energy transfer (NSET) may also occur between CDs and NMs. According to the Persson theory, NSET involves an interband electron transition rather than a resonant interaction between the electrons, which possesses longer energy transfer distance than FRET. Safavi et al. prepared a  $\text{Au}_{0.4}\text{Ag}_{0.6}\text{@C-dots}$  ensemble for  $\text{Cl}^-$  assays via a dual read-out pathway (colorimetric pathway and fluorescent route) [117]. In the fluorescent route, C-dots as donors and alloyed bimetallic Au-Ag nanoparticles as acceptors were used to construct an energy transfer pair through NSET pathway. The emission band of C-dots overlapped with absorption band of alloy bimetals, leading to the fluorescent quenching of C-dots. In the presence of  $\text{Cl}^-$ , the Ag in alloy bimetals would be removed. Hence, the absorption band of alloy bimetals was red shifted, consequently reducing the overlapping between donor and acceptor pairs and recovering the fluorescence signal of C-dots.

#### 4.3.2. Colorimetric detection

Another application of NMs/CDs nanohybrids in sensing is relied on the change in the SPR absorption of NMs, thereby realizing a colorimetric detection. In these sensing systems, the principle was related to the aggregation or re-dispersion of NMs, accompanied by a shift of SPR adsorption of noble metal NP and the change of color. According to previous reports, it can be found that the interaction of functionalized CDs and target pollutants could lead to the aggregation of NMs, which results in a shift of SPR adsorption and the change of color [128,129]. For instance, Safavi et al. established core-shell system Au NPs@S-C-dots for the colorimetric assaying of heavy metal  $\text{Hg}^{2+}$  [129]. As a functionalized material, C-dots doping with S atoms would induce the target  $\text{Hg}^{2+}$  interact with S-C-dots, promoting the shedding of S-C-dots from the Au NPs surface and thus leading to the aggregation of Au NPs accompanied with solution color change from red to blue. Similarly, a colorimetric system CDs-Ag NPs for  $\text{Cu}^{2+}$  detection was subsequently established by Beiraghi et al [61], which was also based on the

interaction of  $\text{Cu}^{2+}$  and functionalized CDs with  $-\text{NH}_2$  and  $-\text{COOH}$ , resulting in the aggregation of Ag NPs (Fig. 8A). In addition, the interaction of NMs and target pollutants also lead to aggregation of NMs [73,82,130]. Luo et al. have fabricated a stable Ag NPs/CQDs composite, providing a sensing platform for colorimetric method for  $\text{Hg}^{2+}$  detection [73]. The target pollutants  $\text{Hg}^{2+}$  interacted with Ag, forming Ag-Hg amalgam and resulting in a decrease in absorbance and shift of SPR band of Ag/CQDs composite accompanied with the color change, which was suitable for colorimetric detection for determination of pollutants.

#### 4.3.3. Electrochemical detection

Recently, the modified electrode with NMs/CDs nanohybrids has become as an effective and versatile electrochemical sensor based on excellent electrocatalytic activity [131,132], which has been applied to detect the pollutants successfully. As for anions, such as  $\text{NO}_2^-$  and  $\text{SO}_3^{2-}$ , the detection mechanism is usually based on the catalytic oxidation of anions by NMs/CDs nanohybrids. For instance, Liu and coworkers have reported an electrochemical platform for  $\text{NO}_2^-$  detection based on Ag/CDs modified on glassy carbon electrode (GCE) [131]. They investigated the electrochemical oxidation of  $\text{NaNO}_2$  at Ag/CDs modified on GCE by cyclic voltammetry, and found the oxidation peak intensity was obvious in comparison of the bare GCE, indicating that Ag/CDs/GCE displayed well electrocatalytic for  $\text{NO}_2^-$  oxidation. Hence, the synergistic effect of Ag/CDs made the appearance of oxidation peak, realizing the detection of  $\text{NO}_2^-$ . Similarly, Zhuang et al. fabricated an electrochemical platform based on CD/Au nanohybrids modified GCE [133]. It showed a higher sensitivity toward the detection of  $\text{NO}_2^-$  with a linear range from 0.1 to 2000  $\mu\text{M}$  and a low detection limit of 0.06  $\mu\text{M}$ . The enhancement of the electrochemical activities for detecting  $\text{NO}_2^-$  could be attributed to well electron transfer and synergistic effect of Au and CDs. Hence, benefiting from the good conductivity and excellent catalytic performance, the modified electrode with NMs/CDs showed a suitable platform for pollutants detection.

Furthermore, the electrochemiluminescence (ECL) sensors based on NMs/CDs for pollutants detection also have been reported successively [64,134], which are smart combination of electrochemistry and chemiluminescence and show low background noise and wide response range [135–137]. For instance, Wang et al. have fabricated a highly sensitive ECL sensor based on the Ag@CQDs composite in aqueous media with  $\text{K}_2\text{S}_2\text{O}_8$  as a coreactant [135]. The mechanism was due to electron transfer annihilation between a quantum dot radical ( $\text{R}^\bullet$ ) and the electrogenerated  $\text{SO}_4^{\bullet-}$ , which was induced by Ag@CQDs. Upon polarization by a negative potential, Ag@CQDs $^-$  was formed by the reduction of Ag@CQDs on electrode, while the strong oxidant  $\text{SO}_4^{\bullet-}$  was formed by the reduction of coreactant  $\text{S}_2\text{O}_8^{2-}$ . Then, the formed  $\text{SO}_4^{\bullet-}$  reacted with electronegative Ag@CQDs $^-$  via electron transfer to generate the excited state Ag@CQDs\*, thus emitting the light. When detecting  $\text{Cl}^-$ ,  $\text{Cl}^-$  would interact with  $\text{Ag}^+$  to form AgCl on the Ag@CQDs. It would weaken the bonding of Ag@CQDs and decrease the conductivity, hence decreasing the ECL intensity of Ag@CQDs (Fig. 8B and C). The critical points in taking NMs/CDs as effective signal probes in an ECL system may lie in how to enhance the ECL intensity and immobilize the NMs/CDs well. Hence, heteroatoms can be doped in CDs to promote the ECL intensity and enhance the interaction between NMs/CDs and electrode [138]. Chai et al. has reported an ECL biosensor serving N-CDs as luminophores and bimetallic Pd-Au hexoctahedrons (Pd@Au HOHs) as enhancers for detecting  $\text{Pb}^{2+}$  with  $\text{K}_2\text{S}_2\text{O}_8$  as a coreactant [139], which not only displayed high sensitivity and accuracy for the detection of  $\text{Pb}^{2+}$ , but also promoted the ECL signal of N-CDs. As discussed above in 3.1.1, most NMs (Ag and Au) have a powerful quenching effect on CDs fluorescence owing to energy transfer between them, while the NMs in these works greatly promoted the ECL intensity of CDs. A reason for this may be that the absorption spectrum of NMs does not overlap well with the ECL spectrum of CDs, which might not cause obvious energy transfer between NMs and CDs. Hence,

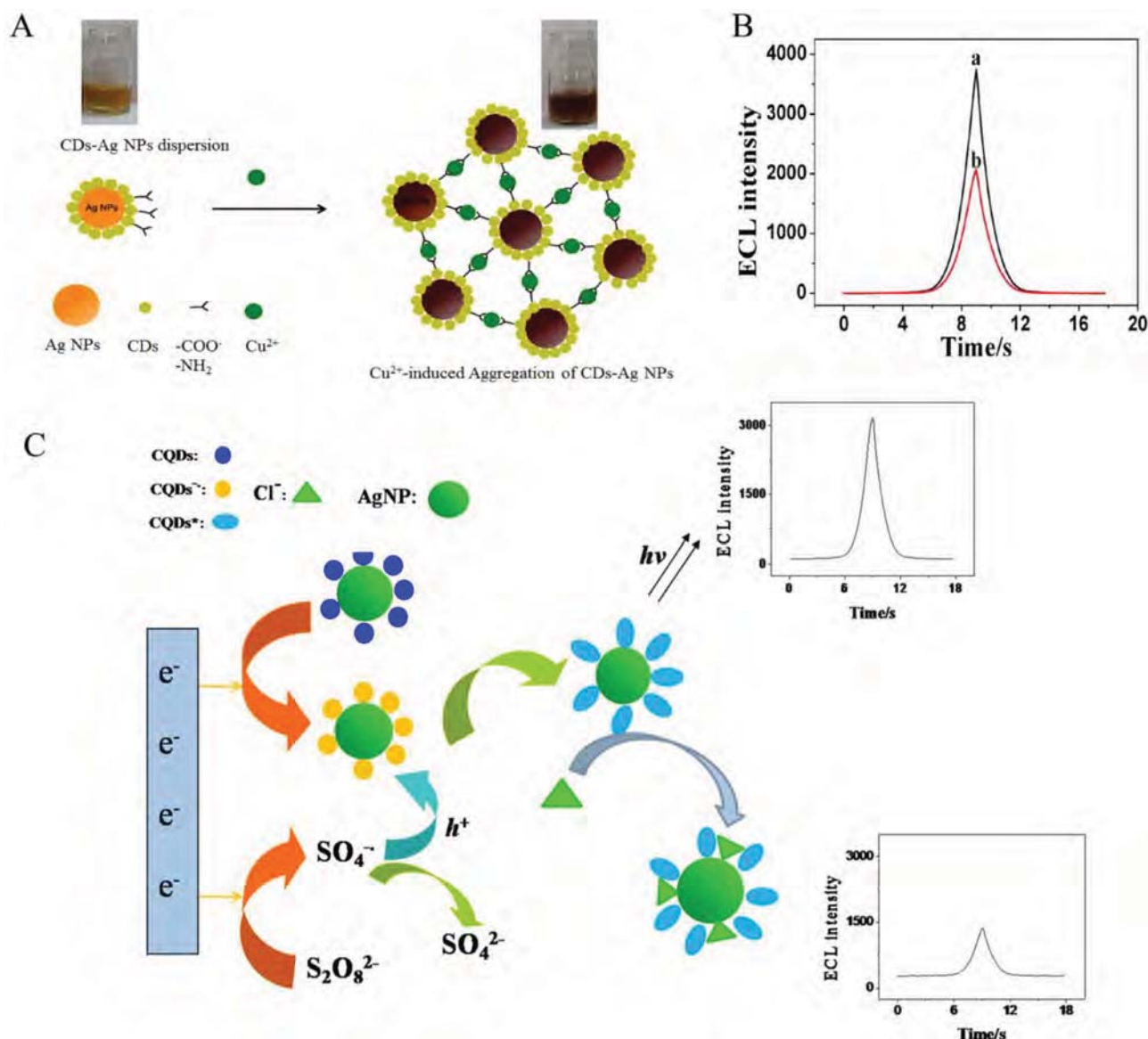


Fig. 8. (A) The detection mechanism of  $\text{Cu}^{2+}$  by colorimetric system CDs-Ag NPs. Reprinted from Ref. [61] with permission from Elsevier. (B) The ECL intensity of Ag@CQDs/GCE. (C) The ECL emission and detection mechanism for  $\text{Cl}^-$  by Ag@CQDs. Reprinted from Ref. [135] with permission from Elsevier.

the ECL signal would not be quenched. In turn, NMs in these works not only promoted the electron transfer, but also effectively catalyzed the oxidation reaction of  $\text{S}_2\text{O}_8^{2-}$  to generate  $\text{SO}_4^{\cdot -}$ , leading to the obvious ECL signal of CDs. When detecting corresponding pollutants, the ECL signal would be quenched by these pollutants.

## 5. Energy-Related applications

### 5.1. Photocatalytic hydrogen evolution and $\text{CO}_2$ reduction

Hydrogen ( $\text{H}_2$ ), as the simplest and most attractive fuel for production, possesses high energy density of  $140 \text{ MJ kg}^{-1}$  [140]. The photocatalytic water splitting into  $\text{H}_2$  and oxygen ( $\text{O}_2$ ) is a direct solar-to-chemical energy conversion technology and has become research hotspot in global [141]. Photocatalytic  $\text{H}_2$  production usually goes through a route that photoexcited electrons reduce the protons in solution to hydrogen atom chemisorbed on catalyst surface and then desorbed into  $\text{H}_2$  [142,143]. At present, NMs/CDs have been used as photocatalysts in energy conversion. In general, noble metal Pt is usually employed as co-catalysts to enhance photocatalytic

performance of CDs [144]. In NMs/CDs, CDs play an important role in harvesting light, which absorb solar photons, facilitate them change into energetic electrons, and transfer electrons. Then, the electrons transferred onto the Pt clusters to reduce  $\text{H}^+$  to  $\text{H}_2$  (Fig. 9A). In a study by Yu et al., photocatalytic  $\text{H}_2$  production was investigated under visible light irradiation using triethanolamine as sacrificial donor by  $\text{ZnIn}_2\text{S}_4$  microspheres (ZIS MSs) co-decorated with CQDs and Pt (Pt/C-ZIS) [145]. Compared to pristine ZIS, Pt loaded ZIS, and CQDs-decorated ZIS, a significant improvement in  $\text{H}_2$  production rate was highlighted in Pt/C-ZIS composite, which is  $1032.2 \mu\text{mol h}^{-1} \text{g}^{-1}$ . The results displayed that the main influence factors of the  $\text{H}_2$  production rate of Pt/C-ZIS were the optical nature, crystal phase and electronic nature. CQDs and Pt NPs in Pt/C-ZIS can facilitate the light adsorption and enhance the crystallinity of Pt/C-ZIS, resulting in less crystal defects and enhanced electrical conductivity. In addition, the vectorial electrons transfer ( $\text{ZIS} \rightarrow \text{CQDs} \rightarrow \text{Pt}$ ) also contributes to the high  $\text{H}_2$  production rate. Xu and his co-workers synthesized catalysts through loading Pt clusters onto surface-reduced CDs (r-CDs/Pt) for solar  $\text{H}_2$  production [23]. Furthermore, heteroatoms doped (such as S, N, P) could effectively modify the electronic and surface property of CDs



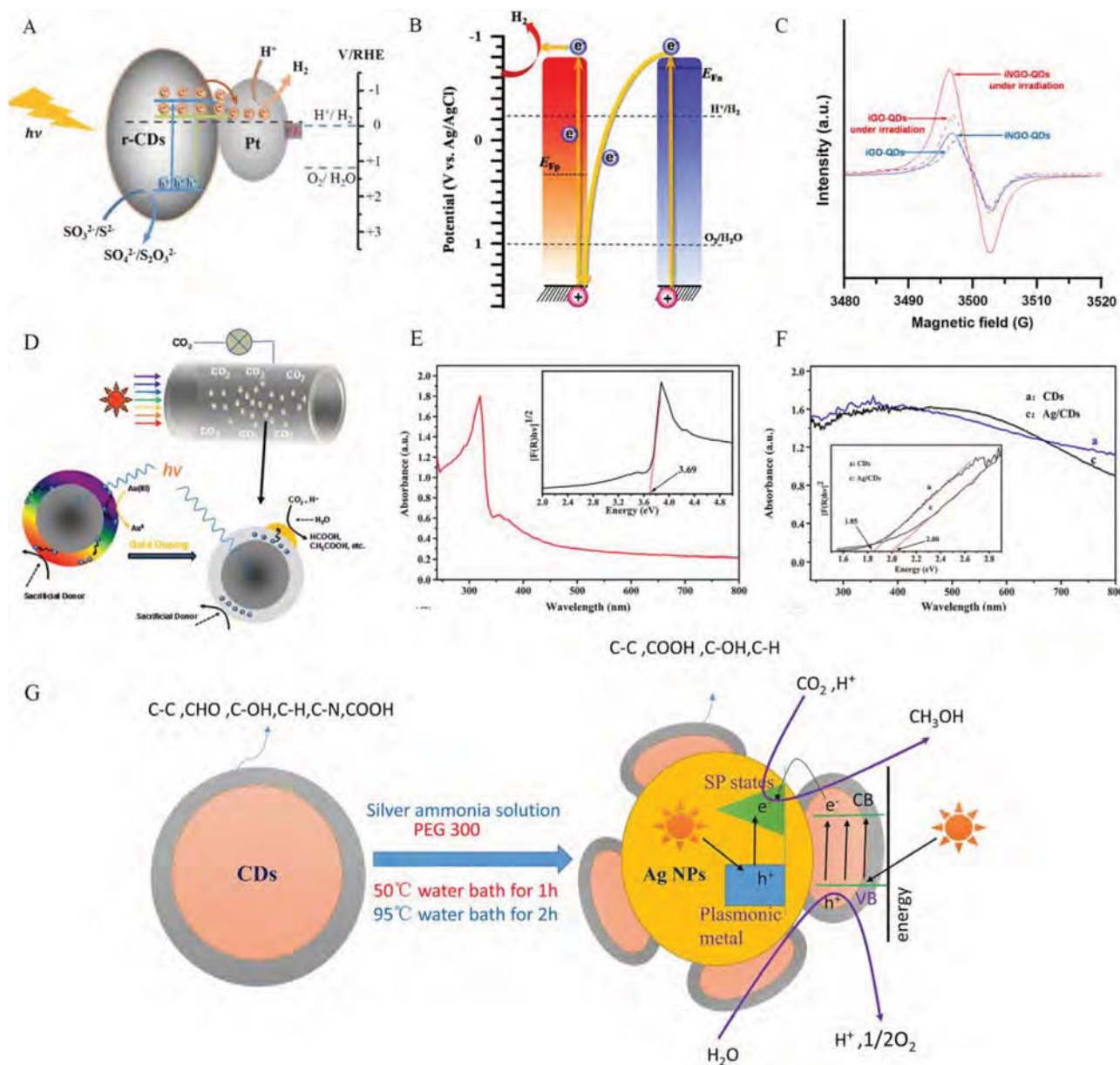


**Fig. 9.** (A) The mechanism of photocatalytic  $H_2$  evolution by r-CD/Pt catalyst. Reprinted from Ref. [23] with permission from Wiley. (B) The mechanism (energy level) of iNGO-QDs with p- and n-type conductivities compared to the potentials for water reduction and oxidation. (C) EPR spectra of the iNGO-QDs and iGO-QDs under the dark and under UV irradiation. Reprinted from Ref. [147] with permission from Elsevier. (D) Mechanism of  $CO_2$  conversion over Au-doped CDs. Reprinted from Ref. [149] with permission from American Chemical Society. UV-vis-NIR diffuse reflectance spectra of (E) Ag (inset: the calculation of bandgap) and (F) Ag and Ag/CDs (inset: the calculation of bandgap). (G) The mechanisms of formation and  $CO_2$  reduction of Ag/CDs. Reprinted from Ref. [94] with permission from Wiley.

[93,103]. For example, the N doped in CDs is prone to donate its lone-pair electrons to conjugate with the aromatic  $\pi$ -orbital electrons on CDs, thus promoting the delocalization of the photogenerated charges and prolonging the lifetime [146]. As to S doping on CDs, S tends to interact with oxygen functional groups during sulfurization, thus passivating charge recombination sites. Teng et al. synthesized surface intact N-doped graphene oxide quantum dots (iNGO-QDs) for Pt depositing, and the photocatalytic activity for  $H_2$  production of the composites was satisfying under visible light irradiation [147], which was excelled to that of  $g-C_3N_4$  and most metal-containing photocatalysts. The N doping in iGO-QDs repaired the vacancy-type defects and brought n-type conductivity to compensate for the unbalanced charges on p-type CDs (Fig. 9B), thereby making full use of photogenerated charges [144]. Under UV light irradiation, the iNGO-QDs displayed an enhanced signal of EPR than that of iGO-QDs, indicating

the high efficiency of the iNGO-QDs towards charges separation, which was demonstrated by the EPR spectra (Fig. 9C). In the process of photocatalytic  $H_2$  evolution, the iNGO-QDs were much more active than iGO-QDs after Pt deposition, confirming the impact of N doping in iNGO-QDs. Besides, they synthesized the S and N co-doped GQDs (A-SNGODs) and then deposited Pt on A-SNGODs, which exhibited enhanced  $H_2$  production efficiency [146].

Zeng and his co-workers deposited Ag NPs on CQDs/ $g-C_3N_4$  by chemical reduction method to employ photocatalytic  $H_2$  generation [148]. The Ag/CQDs/ $g-C_3N_4$  displayed enhanced catalytic activity in  $H_2$  evolution ( $626.93 \mu mol g^{-1} h^{-1}$ ) using triethanolamine as sacrificial agent in contrast to pristine  $g-C_3N_4$  with the feeble  $H_2$  generation ( $94.23 \mu mol g^{-1} h^{-1}$ ). And the apparent quantum efficiency achieved 4.8% under monochromatic lights ( $\lambda = 400 nm$ ). The investigation concluded that the main influence factor for visible-light-driven protons

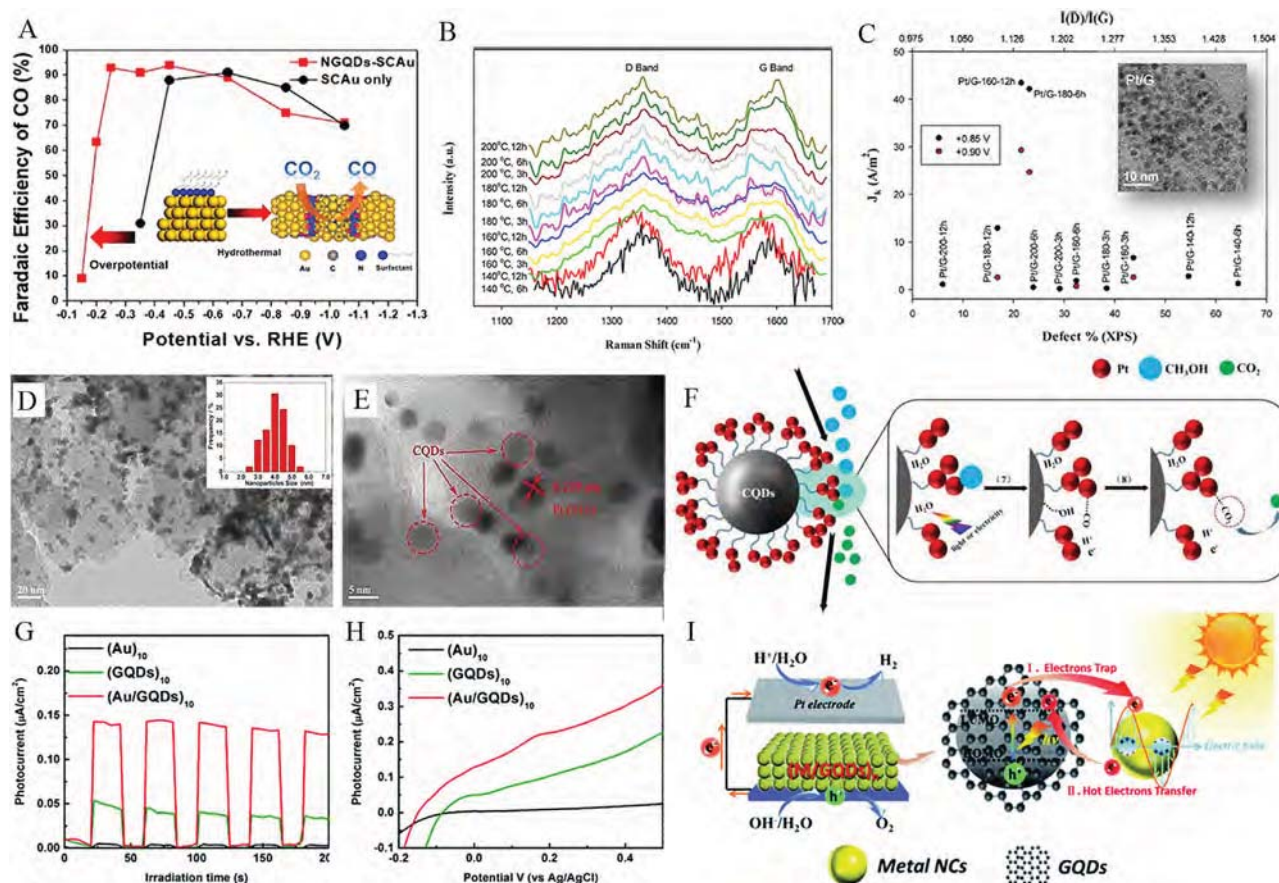


**Fig. 10.** (A) Faradaic efficiency for electrocatalytic conversion of CO<sub>2</sub> to CO over SC Au with or without NGQD coating. Reprinted from Ref. [55] with permission from American Chemical Society. (B) Raman spectra of Pt/GQD prepared under different temperatures. (C) ORR kinetic current density under +0.85 and +0.90 V with GQD defects. Reprinted from Ref. [53] with permission from American Chemical Society. (D) TEM and (E) HRTEM images of Pt/XC-72-CQDs. (F) The mechanism of CQDs for H<sub>2</sub>O activation and chemisorbed CO oxidation. Reprinted from Ref. [151] with permission from Elsevier. (G) On-off transient photocurrent responses and (H) Linear-sweep voltammograms of (Au)<sub>10</sub>, (GQDs)<sub>10</sub> and (Au/GQDs)<sub>10</sub> films. (I) PEC water splitting mechanisms of the (Au/GQDs)<sub>n</sub> films. Reprinted from Ref. [39] with permission from Royal Society of Chemistry.

reduction was the synergistic effect of CQDs, Ag NPs and g-C<sub>3</sub>N<sub>4</sub>. Namely, the Ag NPs and CQDs captured photons with wavelength shorter 550 nm and longer 550 nm, respectively, thereby promoting the generation of photoexcited charge carriers under broad spectrum range. Afterwards, the formed electromagnetic fields and Mott-Schottky junction promoted photogenerated electron transfer, resulting in outstanding protons reduction capacity.

In addition to the photocatalytic H<sub>2</sub> production, NMs/CDs have also been used to catalyze CO<sub>2</sub> reduction to short chain hydrocarbons, which is regarded as a challenging but promising application for energy conversion to settle the energy crisis and climate change. The first example was that poly(ethyleneglycol)diamine (PEG)-passivated CDs coated with noble metals Au or Pt NPs catalyzed CO<sub>2</sub> reduction to form formic acid using isopropanol as the sacrificial agent [78]. CDs were synthesized by oxidation of carbon powders followed by functionalization with PEG, and then coated with Au or Pt NPs via photoreduction. CDs were directly used to absorb solar photons to trigger the photocatalytic reduction reaction, and Au or Pt NPs were used as an electron sink to soak up surface-confined electrons and impede the charges combination. After the pioneering study, the same group further synthesized better-controlled Au coated CDs as catalysts for a closer investigation of the CO<sub>2</sub> reduction [149,150]. The photocatalytic CO<sub>2</sub> reduction over Au-doped carbon dots was employed at ambient temperature with high pressure. As shown in Fig. 9D, the photoexcitation of CDs lead to efficient charge separation, generating electrons at CDs surface and thus helping the reductive formation of Au<sup>3+</sup>. Most

importantly, the formed Au NPs could obviously gather and collect the photogenerated electrons in the CDs, thus enhancing the photocatalytic activities. More recently, Ag NPs/CDs composites were fabricated to catalyze the reduction of CO<sub>2</sub> to CH<sub>3</sub>OH [94]. As shown in Fig. 9E and F, the optical absorption range of Ag NPs/CDs composites was broadened and the bandgap decreased in comparison to single Ag, which improved the photoresponse and promoted generating more electron-hole pairs. Compared to pure Ag or CDs, Ag NPs/CDs composites exhibited almost 3-fold yield of CH<sub>3</sub>OH under 10 h visible light irradiation. The good catalytic activity was because Ag played an important role in extending absorption spectra and CDs possessed excellent electron transfer ability, impeding the combination of charge carriers (Fig. 9G) [1,94].

## 5.2. Electrocatalytic water splitting, oxygen reduction reaction and methanol oxidation reaction

Electrochemical water splitting including oxygen evolution reaction (OER)/hydrogen evolution reaction (HER), and oxygen reduction reaction (ORR) are vital processes for directly converting electric power to chemical energy. Noble metal catalysts (Pt, Ru etc.) were usually used to overcome the intrinsic high kinetic barriers in electrocatalytic reaction. However, the development of electrocatalysis for pure noble metal catalysts are usually impeded by their scarcity and high cost. In view of this, noble metal catalysts have been combined with CDs to develop efficient electrocatalysts [38,58,151].



As discussed above, the combination of NMs and CDs could provide well-dispersivity of NMs and promote electron transfer, which played vital roles in catalytic reaction. Luo et al. designed an electrocatalyst by synergistic coupling of Au and GQDs with a core-shell structure (GQDs-Au) [152], which showed much higher electrocatalytic activity than pristine Au NPs or GQDs and high durability for 1000 cycles. It could be ascribed to the strong interactions between Au NPs and GQDs, in which CQDs coated on Au surface could prevent Au NPs from aggregating and facilitate the electron transfer. Recently, Yang et al. prepared ruthenium nanoparticles/carbon dots (Ru@CQDs) catalysts via pyrolysis method [86]. The catalysts exhibited a boosted HER catalytic activity in alkaline condition, and the onset overpotential was 0 mV. The density functional theory (DFT) calculations indicated a synergistic effect between Ru and N-doped CQDs to facilitate H<sub>2</sub>O adsorption and dissociation. The integration of Ru and CQDs made the charge density redistribute, which was conducive to the electrons transfer from Ru to CQDs. It would make electron enriched in CQDs and hole enriched in Ru and enhance the charge separation [153]. In another report, Li et al. prepared N-doped GQDs-wrapped single crystalline Au NPs (NGQDs-SCAu NPs) for converting CO<sub>2</sub> to CO [55]. The onset potential reached as low as 0.15 V (vs.RHE), corresponding to a significantly improved overpotential of only 0.04 V (Fig. 10A).

Fuel cells are efficient tools to transform chemical energy to electrical energy. The key to improve the conversion efficiency is to overcome the sluggish electron-transfer kinetics of ORR at fuel cell cathode [154,155]. One of the methods is to design the oxygenated defects in GQDs. For examples, Chen's groups fabricated GQDs with oxygenated defectes-supported platinum nanoparticles (Pt/G) for ORR, which showed marked catalytic activity with an onset potential of + 1.05 V. This was about 70 mV more positive than that of commercial Pt/C nanoparticles [156]. The same group further developed GQDs-supported palladium NPs (Pd/GQD) [154]. These studies reported the enhanced activity for ORR activity over GQD-supported Pt and the synergistic effect between two components [53,156,157]. As shown in Fig. 10B and C, the ORR activity changed with GQD defect concentration with volcanic shaped form. Hence, the high activity was related to the manipulation of oxygenated defects of GQD. GQD defects could not only promote the charge transfer from NMs to GQDs, thereby lowering the activation energy for O<sub>2</sub> dissociation, but also decreased the energy barrier by weakening the binding oxygen intermediate, thereby accelerating the ORR reaction [158]. It could also provide natural sites for noble metal anchoring, improving the dispersivity of NMs and allowing for intimate interaction between NMs and supports [53,71,159]. In addition to design oxygenated defects in GQDs, another approach was that heteroatoms could be doped into GQDs to enhance the electrochemical activity [83,160-163]. In their following study, N-doped GQDs were prepared for supporting palladium nanoparticles (Pd/NGQDs), which exhibited apparent electrocatalytic activity for ORR [164].

The kinetic rate of methanol oxidation reaction (MOR) in fuel cell anode is also important for converting chemical energy to electric energy [58,165,166]. Li et al. prepared Pt/N-doped CQDs (Pt/N-CQDs) through a simple chemical method using rice husk-based carbon derived N-CQDs [157]. N-CQDs with a large specific surface area and a certain amounts of defects could provide more active sites to facilitate Pt uniformly anchoring, resulting in high utilization of Pt. In another report, Pt assisted by CQDs (Pt/XC-72-CQDs) hybrids were also synthesized through a simple chemical reduction, which showed superior activity and stability for the MOR due to the synergistic effect of Pt and CQDs [151]. Herein, CQDs not only facilitated Pt uniformly anchoring (Fig. 10D and E), but also provided a rapid route to activate water, thus promoting the conversion rate of intermediates CO to CO<sub>2</sub>, which prevented Pt from poison by CO (Fig. 10F). Recently, Au-GQDs@Pt core-shell nanodendrites were synthesized for MOR by Zhou et al [95], which exhibited high electrocatalysis and anti-CO poisoning ability. They found the mole ratios of Au and Pt would affect the Pt shell

thickness, which would further influence the catalytic activity.

### 5.3. Photoelectrochemical catalytic reaction

Benefiting from SPR effect and high activity of NMs as well as up-conversion and unique electron properties of CDs, NMs/CDs are also employed in photoelectrochemical (PEC) water splitting and MOR [153]. The mechanism of NMs/CDs in PEC water splitting was detailed by Zeng's group [39,56]. They prepared (Au/GQDs)<sub>10</sub> films for PEC water splitting, exhibiting remarkable catalytic performance. The photocurrent of (Au/GQDs)<sub>10</sub> films was much higher than that of (Au)<sub>10</sub> films and (GQDs)<sub>10</sub> films (Fig. 10G). No photocurrent was detected in (Au)<sub>10</sub> films, but photocurrent was detected in (Au/GQDs)<sub>10</sub> films with almost 3-fold higher than that of (GQDs)<sub>10</sub> films. Similar trends were also found in the linear-sweep voltammograms results in the different multilayer films (Fig. 10H). It exhibited a more effective separation of photogenerated charge carriers over (Au/GQDs)<sub>10</sub> films, in which GQDs mainly produced the photogenerated electron-hole pairs during light irradiation and employed as a semiconductor for band-gap photo-excitation, and Au NPs mainly played double roles of SPR photosensitizer for producing hot electrons and electrons sink for capturing photogenerated electrons from GQDs (Fig. 10I). Hence, the cooperative synergy of Au and GQDs for photocurrent generation and enhancement was confirmed. In addition, Dolui et al. also designed a CDs sensitized TiO<sub>2</sub> supported Pt catalyst for photoelectrocatalytic MOR [167]. Benefitting from the up-conversion property of CDs and high electrocatalytic activity of Pt, the catalyst exhibited high catalytic activity, well CO poison tolerance and stability.

## 6. Conclusions and challenges

In summary, the NMs/CDs hybrids have been studied in many fields owing to their enhanced properties. Herein, we have presented an overview of NMs/CDs hybrids, focusing on their synthetic methods, physicochemical characterizations, environment-related (detection and treatment) and energy-related applications (water splitting, ORR and MOR), as well as the mechanism in their synergistic effect. Generally, the NMs/CDs can be synthesized via chemical reduction, hydrothermal method and assembled method. And the physicochemical characterizations mainly involve optical properties, photochemistry, and surface chemistry characterization, and microscopy characterization. The detection performance and catalytic activity of NMs/CDs are all greatly enhanced due to the synergistic effect. For the NMs/CDs in detection applications, the unique optical, electronic, and fluorescence properties of NMs/CDs create the conditions for constructing multiple detection systems. For instance, NMs could enhance the fluorescence of CDs via a metal-enhanced fluorescence technology to promote the sensitive of NMs/CDs based fluorescent detection systems. In addition, NMs combined with CDs could construct the "dual-emission" ratiometric fluorescent sensors owing to the fluorescence of NMs. It provided more distinct color change and accurate measurement without the interference from complicated environment, which surpassed the single-emission probe of CDs. For the NMs/CDs in catalysis applications, commonly, their electron transfer ability is magnified after hybridization, further promoting simultaneous and rapid catalytic degradation of various pollutants or energy conversion. In the photocatalysis, the unique up-conversion of CDs play an important role in harvesting light, which can absorb lower energy photons and facilitate them changing into higher energetic electrons. Then NMs act as electron sink and plasmonic cocatalysts mediated by LSPR, which endow NMs/CDs with enhanced light utilization ability in full spectrum and thereby promoting photocatalytic activity.

Despite the great progress of NMs/CDs in environment-related and energy-related applications, it is believed that there are still at early stages in terms of hybrids synthesis and performance, which remains low for widespread applications. Herein, several important issues are



highlighted to overcome some challenges for future research.

(i) Realizing stable and rapid synthetic methods for NMs/CDs nanohybrids is important. As shown in Table 1, the variety of synthetic methods (top-down and bottom-up methods) of CDs makes strong distinctions on its types and numbers of surface functional groups, thereby making the various particle sizes of NMs and difficult to guarantee the reproducibility of synthetic NMs/CDs composites. Hence, fully understanding the mechanism of synthetic methods and figuring out the impact of some factors (functional groups of CDs, synthetic period and reaction temperature) on synthetic process can help guide the synthesis of NMs/CDs.

(ii) As for NMs/CDs in photocatalysis applications, the roles of NMs and CDs in the hybrids have been illustrated in some examples. But in the photocatalytic materials composed of NMs and CDs (when NMs/CDs combined with other semiconductors), the working mechanism and electron transfer pathway should be further understood. For example, the interface between noble metals and semiconductors may form Schottky barrier. When this process happens, the electron transfer pathway will have some changes. In addition, the LSPR effect of plasmonic noble metals is related to the size, shape and other parameters, which may also influence electron transfer. Hence, it is imperative to investigate the mechanism in detail. Some powerful characterization techniques combined with theoretical calculations could be used to reveal the NMs/CDs and clarify the reaction mechanism, such as ion scattering, photoluminescence spectroscopy, DFT and total density of states calculations.

(iii) To further enhance practicality and accessibility of NMs/CDs in detection pollutants applications, the detection systems using NMs/CDs can be fabricated to portable and miniaturized systems. For example, fabricating NMs/CDs hybrids probes on substrates such as paper strips are expected to be developed for convenient and sensitive in situ detection of pollutants.

(iv) Recovery of NMs/CDs nanohybrids to separate from aqueous solution is another challenge. Magnetic nanomaterials can be combined with the nanohybrids for improving their separation in water treatment, which deserve further study. At present, there have been some studies about the NMs/CDs combined with magnetic materials. But it should be noticed that the stability and dispersivity of NMs and CDs on the surface of magnetic materials are extremely important, which would affect the performance of NMs/CDs.

(v) High price and low abundance of NMs limit the practical application of NMs/CDs. Hence, further boosting the performance of NMs/CDs and reducing dosage of NMs in NMs/CDs could be considered to reduce the cost. On one hand, the performance and stability of NMs/CDs can be further enhanced by rational designing the structure of NMs/CDs or combining NMs/CDs with other nanomaterials, thereby reducing the cost. For instance, anisotropic NMs with sharp edges and corners display better catalytic activity, which is superior to NMs with circular shape. Hence, rational designing the anisotropic NMs with CDs may greatly enhance the performance of NMs/CDs. On the other hand, NMs could combine or even be replaced with suitable base metals to reduce the dosage of NMs. In addition, single-atom NMs with higher activity may be used to reduce the dosage of NMs. However, the single-atom deposition technique is far from mature. But it is an orientation to develop for maximizing the utilization efficiency of scarce precious NMs, and more effort need to exploit for the technique development. We believe that there will be suitable cost and technical maturity of single-atom deposition technique with researchers' continuous exploration.

(vi) Compared with other carbon-based nanohybrids, the energy-related application of NMs/CDs nanohybrids is less promising. Hence, for practical application, people may pursue other more effective nanohybrids rather than the CDs based nanohybrids. So, more efforts and study need to exploit for further revealing their mechanism and thereby improving the performance and practical applications of NMs/CDs nanohybrids.

Although multifunctional NMs/CDs nanohybrids exhibit well performance in various applications, the obtained NMs/CDs nanohybrids are still far from suitable for practical applications. Overall, persistent studies toward NMs/CDs in synthesis, characterization and mechanistic understanding are needed to fully exploit and effectively apply NMs/CDs in catalysis and detection applications. The efforts made on the exploration of NMs/CDs can bring some breakthroughs in the understanding of the mechanism behind on the hybrids, and help develop more combinations of nanomaterials.

## Declaration of Competing Interest

The authors declare that they have no known competing financial interests or personal relationships that could have appeared to influence the work reported in this paper.

## Acknowledgements

This study was financially supported by the Program for the National Natural Science Foundation of China (51879101, 51579098, 51779090, 51709101, 51521006, 51809090, 51909084), the National Program for Support of Top-Notch Young Professionals of China (2014), the Program for Changjiang Scholars and Innovative Research Team in University (IRT-13R17), and Hunan Provincial Science and Technology Plan Project (2018SK20410, 2017SK2243, 2016RS3026), and the Fundamental Research Funds for the Central Universities (531119200086, 531118010114, 531107050978, 541109060031, 531118010473), and the Three Gorges Follow-up Research Project (2017HXXY-05).

## References

- [1] S. Gogoi, N. Karak, Solar-Driven Hydrogen Peroxide Production Using Polymer-Supported Carbon Dots as Heterogeneous Catalyst, *Nano-Micro Letters* 9 (2017) 40.
- [2] L. Qin, D. Huang, P. Xu, G. Zeng, C. Lai, Y. Fu, H. Yi, B. Li, C. Zhang, M. Cheng, C. Zhou, X. Wen, In-situ deposition of gold nanoparticles onto polydopamine-decorated g-C<sub>3</sub>N<sub>4</sub> for highly efficient reduction of nitroaromatics in environmental water purification, *J Colloid Interface Sci* 534 (2019) 357–369.
- [3] C. Wang, D. Astruc, Nanogold plasmonic photocatalysis for organic synthesis and clean energy conversion, *Chem Soc Rev* 43 (2014) 7188–7216.
- [4] P. Zhao, X. Feng, D. Huang, G. Yang, D. Astruc, Basic concepts and recent advances in nitrophenol reduction by gold- and other transition metal nanoparticles, *Coord. Chem. Rev.* 287 (2015) 114–136.
- [5] Y. Fu, L. Qin, D. Huang, G. Zeng, C. Lai, B. Li, J. He, H. Yi, M. Zhang, M. Cheng, X. Wen, Chitosan functionalized activated coke for Au nanoparticles anchoring: Green synthesis and catalytic activities in hydrogenation of nitrophenols and azo dyes, *Appl. Catal. B* 255 (2019) 117740.
- [6] L. Qin, Z. Zeng, G. Zeng, C. Lai, A. Duan, R. Xiao, D. Huang, Y. Fu, H. Yi, B. Li, X. Liu, S. Liu, M. Zhang, D. Jiang, Cooperative catalytic performance of bimetallic Ni-Au nanocatalyst for highly efficient hydrogenation of nitroaromatics and corresponding mechanism insight, *Appl. Catal. B* 259 (2019) 118035.
- [7] L. Qin, H. Yi, G. Zeng, C. Lai, D. Huang, P. Xu, Y. Fu, J. He, B. Li, C. Zhang, M. Cheng, H. Wang, X. Liu, Hierarchical porous carbon material restricted Au catalyst for highly catalytic reduction of nitroaromatics, *J Hazard Mater* 380 (2019) 120864.
- [8] S.E. Kudaibergenov, G.S. Tatykhanova, B.S. Selenova, Polymer Protected and Gel Immobilized Gold and Silver Nanoparticles in Catalysis, *J. Inorg. Organomet. Polym. Mater.* 26 (2016) 1198–1211.
- [9] A. Corma, H. Garcia, Supported gold nanoparticles as catalysts for organic reactions, *Chem Soc Rev* 37 (2008) 2096–2126.
- [10] D. Wang, N.B. Saleh, W. Sun, C.M. Park, C. Shen, N. Aich, W. Peijnenburg, W. Zhang, Y. Jin, C. Su, Next-Generation Multifunctional Carbon-Metal Nanohybrids for Energy and Environmental Applications, *Environ Sci Technol* 53 (2019) 7265–7287.
- [11] X. Gao, C. Du, Z. Zhuang, W. Chen, Carbon quantum dot-based nanoprobes for metal ion detection, *J. Mater. Chem. C* 4 (2016) 6927–6945.
- [12] C. Hu, M. Li, J. Qiu, Y.P. Sun, Design and fabrication of carbon dots for energy conversion and storage, *Chem Soc Rev* 48 (2019) 2315–2337.
- [13] V. Georgakilas, J.A. Perman, J. Tucek, R. Zboril, Broad Family of Carbon Nanoallotropes: Classification, Chemistry, and Applications of Fullerenes, Carbon Dots, Nanotubes, Graphene, Nanodiamonds, and Combined Superstructures, *Chem. Rev.* 115 (2015) 4744–4822.
- [14] J. Liu, H. Xu, Y. Xu, Y. Song, J. Lian, Y. Zhao, L. Wang, L. Huang, H. Ji, H. Li, Graphene quantum dots modified mesoporous graphite carbon nitride with

- significant enhancement of photocatalytic activity, *Appl. Catal. B* 207 (2017) 429–437.
- [15] H. Wang, Z. Wei, H. Matsui, S. Zhou,  $\text{Fe}_3\text{O}_4$ /carbon quantum dots hybrid nano-flowers for highly active and recyclable visible-light driven photocatalyst, *J. Mater. Chem. A* 2 (2014) 15740–15745.
- [16] X. Guo, Q. Liu, J. Liu, H. Zhang, J. Yu, R. Chen, D. Song, R. Li, J. Wang, Magnetic metal-organic frameworks/carbon dots as a multifunctional platform for detection and removal of uranium, *Appl. Surf. Sci.* 491 (2019) 640–649.
- [17] Y. Ali, V.-T. Nguyen, N.-A. Nguyen, S. Shin, H.-S. Choi, Transition-metal-based  $\text{NiCoS}/\text{C}$ -dot nanoflower as a stable electrocatalyst for hydrogen evolution reaction, *Int. J. Hydrogen Energy* 44 (2019) 8214–8222.
- [18] Y. Jiao, Q. Huang, J. Wang, Z. He, Z. Li, A novel  $\text{MoS}_2$  quantum dots (QDs) decorated Z-scheme g-C $_3\text{N}_4$  nanosheet/N-doped carbon dots heterostructure photocatalyst for photocatalytic hydrogen evolution, *Appl. Catal. B* 247 (2019) 124–132.
- [19] L. Wang, Y. Li, S. Li, Y. Wang, W. Kong, W. Xue, C. Li, Synthesis, characterization and photocatalytic activity of graphene quantum dots-Ag solar driven photocatalyst, *J. Mater. Sci.: Mater. Electron.* 28 (2017) 17570–17577.
- [20] A.N. Emam, A.A. Mostafa, M.B. Mohamed, A.S. Gadallah, M. El-Kemary, Enhancement of the Collective Optical Properties of Plasmonic Hybrid Carbon Dots via Localized Surface Plasmon, *J. Lumin.* 200 (2018) 287–297.
- [21] J. Ju, W. Chen, In situ growth of surfactant-free gold nanoparticles on nitrogen-doped graphene quantum dots for electrochemical detection of hydrogen peroxide in biological environments, *Anal. Chem.* 87 (2015) 1903–1910.
- [22] C. Wu, Y. Yuan, Q. He, R. Song, Two-step synthesis of Ag@GQD hybrid with enhanced photothermal effect and catalytic performance, *Nanotechnology* 27 (2016) 48LT02.
- [23] X. Xu, W. Tang, Y. Zhou, Z. Bao, Y. Su, J. Hu, H. Zeng, Steering Photoelectrons Excited in Carbon Dots into Platinum Cluster Catalyst for Solar-Driven Hydrogen Production, *Adv. Sci. (Weinh.)* 4 (2017) 1700273.
- [24] Y. Li, X. Fan, J. Qi, J. Ji, S. Wang, G. Zhang, F. Zhang, Gold nanoparticles–graphene hybrids as active catalysts for Suzuki reaction, *Mater. Res. Bull.* 45 (2010) 1413–1418.
- [25] I.F. Teixeira, E.C.M. Barbosa, S.C.E. Tsang, P.H.C. Camargo, Carbon nitrides and metal nanoparticles: from controlled synthesis to design principles for improved photocatalysis, *Chem. Soc. Rev.* 47 (2018) 7783–7817.
- [26] Y. Cheng, Y. Fan, Y. Pei, M. Qiao, Graphene-supported metal/metal oxide nanohybrids: synthesis and applications in heterogeneous catalysis, *Catal. Sci. Technol.* 5 (2015) 3903–3916.
- [27] S. Mallakpour, E. Khadem, Carbon nanotube–metal oxide nanocomposites: Fabrication, properties and applications, *Chem. Eng. J.* 302 (2016) 344–367.
- [28] M.J. Molaei, The optical properties and solar energy conversion applications of carbon quantum dots: A review, *Sol. Energy* 196 (2020) 549–566.
- [29] Z. Zhu, Y. Zhai, Z. Li, P. Zhu, S. Mao, C. Zhu, D. Du, L.A. Belfiore, J. Tang, Y. Lin, Red carbon dots: Optical property regulations and applications, *Mater. Today* 30 (2019) 52–79.
- [30] M. Hassan, V.G. Gomes, A. Dehghani, S.M. Ardekani, Engineering carbon quantum dots for photomediated theranostics, *Nano Res.* 11 (2017) 1–41.
- [31] Z. Li, L. Wang, Y. Li, Y. Feng, W. Feng, Frontiers in carbon dots: design, properties and applications, *Mater. Chem. Front.* 3 (2019) 2571–2601.
- [32] Y. Wang, A. Hu, Carbon quantum dots: synthesis, properties and applications, *J. Mater. Chem. C* 2 (2014) 6921.
- [33] Y. Yang, C. Zhang, D. Huang, G. Zeng, J. Huang, C. Lai, C. Zhou, W. Wang, H. Guo, W. Xue, Boron nitride quantum dots decorated ultrathin porous g-C $_3\text{N}_4$ : intensified exciton dissociation and charge transfer for promoting visible-light-driven molecular oxygen activation, *Appl. Catal. B* 245 (2019) 87–99.
- [34] M. Han, S. Zhu, S. Lu, Y. Song, T. Feng, S. Tao, J. Liu, B. Yang, Recent progress on the photocatalysis of carbon dots: Classification, mechanism and applications, *Nano Today* 19 (2018) 201–218.
- [35] S. Sun, Y. Wang, L.n. Wang, T. Guo, X. Yuan, D. Zhang, Z. Xue, X. Zhou, X. Lu, Synthesis of Au@nitrogen-doped carbon quantum dots@Pt core-shell structure nanoparticles for enhanced methanol electrooxidation, *J. Alloy. Compd.* 793 (2019) 635–645.
- [36] X. Hu, J. Shi, Y. Shi, X. Zou, M. Arslan, W. Zhang, X. Huang, Z. Li, Y. Xu, Use of a smartphone for visual detection of melamine in milk based on Au@Carbon quantum dots nanocomposites, *Food Chem.* 272 (2019) 58–65.
- [37] M. Gholinejad, C. Najera, F. Hamed, M. Seyedhamzeh, M. Bahrami, M. Kompany-Zareh, Green synthesis of carbon quantum dots from vanillin for modification of magnetite nanoparticles and formation of palladium nanoparticles: Efficient catalyst for Suzuki reaction, *Tetrahedron* 73 (2017) 5585–5592.
- [38] S. Yang, F. Zhang, C. Gao, J. Xia, L. Lu, Z. Wang, A sandwich-like PtCo-graphene/carbon dots/graphene catalyst for efficient methanol oxidation, *J. Electroanal. Chem.* 802 (2017) 27–32.
- [39] Z. Zeng, F.-X. Xiao, H. Phan, S. Chen, Z. Yu, R. Wang, T.-Q. Nguyen, T.T. Yang Tan, Unraveling the cooperative synergy of zero-dimensional graphene quantum dots and metal nanocrystals enabled by layer-by-layer assembly, *J. Mater. Chem. A* 6 (2018) 1700–1713.
- [40] Q. Lu, J. Deng, Y. Hou, H. Wang, H. Li, Y. Zhang, S. Yao, Hydroxyl-rich C-dots synthesized by a one-pot method and their application in the preparation of noble metal nanoparticles, *Chem. Commun.* 51 (2015) 7164–7167.
- [41] J. Chen, H. Che, K. Huang, C. Liu, W. Shi, Fabrication of a ternary plasmonic photocatalyst QDs/Ag/Ag $_2\text{O}$  to harness charge flow for photocatalytic elimination of pollutants, *Appl. Catal. B* 192 (2016) 134–144.
- [42] X. Li, M. Rui, J. Song, Z. Shen, H. Zeng, Carbon and Graphene Quantum Dots for Optoelectronic and Energy Devices: A Review, *Adv. Funct. Mater.* 25 (2015) 4929–4947.
- [43] G.A.M. Hutton, B.C.M. Martindale, E. Reisner, Carbon dots as photosensitisers for solar-driven catalysis, *Chem. Soc. Rev.* 46 (2017) 6111–6123.
- [44] T.P. Araujo, J. Quiroz, E.C.M. Barbosa, P.H.C. Camargo, Understanding plasmonic catalysis with controlled nanomaterials based on catalytic and plasmonic metals, *Curr. Opin. Colloid Interface Sci.* 39 (2019) 110–122.
- [45] M.A. Muhammed, M. Dobliger, J. Rodriguez-Fernandez, Switching Plasmons: Gold Nanorod-Copper Chalcogenide Core-Shell Nanoparticle Clusters with Selectable Metal/Semiconductor NIR Plasmon Resonances, *J. Am. Chem. Soc.* 137 (2015) 11666–11677.
- [46] Q. Yang, Q. Xu, H.L. Jiang, Metal-organic frameworks meet metal nanoparticles: synergistic effect for enhanced catalysis, *Chem. Soc. Rev.* 46 (2017) 4774–4808.
- [47] B. Wu, Y. Kuang, X. Zhang, J. Chen, Noble metal nanoparticles/carbon nanotubes nanohybrids: Synthesis and applications, *Nano Today* 6 (2011) 75–90.
- [48] Y. Fu, P. Xu, D. Huang, G. Zeng, C. Lai, L. Qin, B. Li, J. He, H. Yi, M. Cheng, C. Zhang, Au nanoparticles decorated on activated coke via a facile preparation for efficient catalytic reduction of nitrophenols and azo dyes, *Appl. Surf. Sci.* 473 (2019) 578–588.
- [49] L. Qin, G. Zeng, C. Lai, D. Huang, C. Zhang, P. Xu, T. Hu, X. Liu, M. Cheng, Y. Liu, L. Hu, Y. Zhou, A visual application of gold nanoparticles: Simple, reliable and sensitive detection of kanamycin based on hydrogen-bonding recognition, *Sens. Actuators, B* 243 (2017) 946–954.
- [50] Y. Liu, Y. Zhao, Q. Fan, M.S. Khan, X. Li, Y. Zhang, H. Ma, Q. Wei, Aptamer based electrochemiluminescent thrombin assay using carbon dots anchored onto silver-decorated polydopamine nanospheres, *Mikrochim. Acta* 185 (2018) 85.
- [51] Q. Huang, X. Lin, J.-J. Zhu, Q.-X. Tong, Pd-Au@carbon dots nanocomposite: Facile synthesis and application as an ultrasensitive electrochemical biosensor for determination of colistin DNA in human serum, *Biosens. Bioelectron.* 94 (2017) 507–512.
- [52] Y. Deng, L. Tang, C. Feng, G. Zeng, J. Wang, Y. Lu, Y. Liu, J. Yu, S. Chen, Y. Zhou, Construction of Plasmonic Ag and Nitrogen-Doped Graphene Quantum Dots Decorated Ultrathin Graphitic Carbon Nitride Nanosheet Composites with Enhanced Photocatalytic Activity: Full-Spectrum Response Ability and Mechanism Insight, *ACS Appl. Mater. Interfaces* 9 (2017) 42816–42828.
- [53] Y. Song, S. Chen, Graphene quantum-dot-supported platinum nanoparticles: defect-mediated electrocatalytic activity in oxygen reduction, *ACS Appl. Mater. Interfaces* 6 (2014) 14050–14060.
- [54] K. He, Z. Zeng, A. Chen, G. Zeng, R. Xiao, P. Xu, Z. Huang, J. Shi, L. Hu, G. Chen, Advancement of Ag–graphene based nanocomposites: an overview of synthesis and its applications, *Small* 14 (2018) 1800871.
- [55] J. Fu, Y. Wang, J. Liu, K. Huang, Y. Chen, Y. Li, J.-J. Zhu, Low Overpotential for Electrochemically Reducing  $\text{CO}_2$  to CO on Nitrogen-Doped Graphene Quantum Dots-Wrapped Single-Crystalline Gold Nanoparticles, *ACS Energy Lett.* 3 (2018) 946–951.
- [56] Z. Zeng, Y.-B. Li, S. Chen, P. Chen, F.-X. Xiao, Insight into the charge transport correlation in Au clusters and graphene quantum dots deposited on  $\text{TiO}_2$  nanotubes for photoelectrochemical oxygen evolution, *J. Mater. Chem. A* 6 (2018) 11154–11162.
- [57] H. Choi, S.-J. Ko, Y. Choi, P. Joo, T. Kim, B.R. Lee, J.-W. Jung, H.J. Choi, M. Cha, J.-R. Jeong, I.-W. Hwang, M.H. Song, B.-S. Kim, J.Y. Kim, Versatile surface plasmon resonance of carbon-dot-supported silver nanoparticles in polymer optoelectronic devices, *Nat. Photonics* 7 (2013) 732.
- [58] Z. Li, M. Ruan, L. Du, G. Wen, C. Dong, H.-W. Li, Graphene nanomaterials supported palladium nanoparticles as nanocatalysts for electro-oxidation of methanol, *J. Electroanal. Chem.* 805 (2017) 47–52.
- [59] X.T. Zheng, A. Ananthanarayanan, K.Q. Luo, P. Chen, Glowing graphene quantum dots and carbon dots: properties, syntheses, and biological applications, *Small* 11 (2015) 1620–1636.
- [60] E. Haque, J. Kim, V. Malgras, K.R. Reddy, A.C. Ward, J. You, Y. Bando, M.S.A. Hossain, Y. Yamauchi, Recent Advances in Graphene Quantum Dots: Synthesis, Properties, and Applications, *Small Methods* 2 (2018) 1800050.
- [61] A. Beiraghi, S.A. Najibi-Gehraz, Carbon dots-modified silver nanoparticles as a new colorimetric sensor for selective determination of cupric ions, *Sens. Actuators, B* 253 (2017) 342–351.
- [62] Y. Guo, D. Tang, L. Zhang, B. Li, A. Iqbal, W. Liu, W. Qin, Synthesis of ultrathin carbon dots-coated iron oxide nanocubes decorated with silver nanoparticles and their excellent catalytic properties, *Ceram. Int.* 43 (2017) 7311–7320.
- [63] W. Liu, F. Ding, Y. Wang, L. Mao, R. Liang, P. Zou, X. Wang, Q. Zhao, H. Rao, Fluorometric and colorimetric sensor array for discrimination of glucose using enzymatic-triggered dual-signal system consisting of Au@Ag nanoparticles and carbon nanodots, *Sens. Actuators, B* 265 (2018) 310–317.
- [64] X. Zhao, D. He, Y. Wang, Y. Hu, C. Fu, Au nanoparticles and graphene quantum dots co-modified glassy carbon electrode for catechol sensing, *Chem. Phys. Lett.* 647 (2016) 165–169.
- [65] L. Yang, X. Liu, Q. Lu, N. Huang, M. Liu, Y. Zhang, S. Yao, Catalytic and peroxidase-like activity of carbon based-AuPd bimetallic nanocomposite produced using carbon dots as the reductant, *Anal. Chim. Acta* 930 (2016) 23–30.
- [66] P.J. Babu, A.M. Raichur, M. Doble, Synthesis and characterization of biocompatible carbon-gold (C-Au) nanocomposites and their biomedical applications as an optical sensor for creatinine detection and cellular imaging, *Sens. Actuators, B* 258 (2018) 1267–1278.
- [67] V. Strauss, J.T. Margraf, C. Dolle, B. Butz, T.J. Nacken, J. Walter, W. Bauer, W. Peukert, E. Specker, T. Clark, D.M. Guldi, Carbon Nanodots: Toward a Comprehensive Understanding of Their Photoluminescence, *J. Am. Chem. Soc.* 136 (2014) 17308–17316.
- [68] B. Zheng, X. Liu, Y. Wu, L. Yan, J. Du, J. Dai, Q. Xiong, Y. Guo, D. Xiao, Surfactant-free gold nanoparticles: rapid and green synthesis and their greatly improved

- catalytic activities for 4-nitrophenol reduction, *Inorg. Chem. Front.* 4 (2017) 1268–1272.
- [69] T. Liu, N. Li, J.X. Dong, Y. Zhang, Y.Z. Fan, S.M. Lin, H.Q. Luo, N.B. Li, A colorimetric and fluorometric dual-signal sensor for arginine detection by inhibiting the growth of gold nanoparticles/carbon quantum dots composite, *Biosens. Bioelectron.* 87 (2017) 772–778.
  - [70] K. Iqbal, A. Iqbal, A.M. Kirillov, C. Shan, W. Liu, Y. Tang, A new multicomponent CDs/Ag@Mg–Al–Ce-LDH nanocatalyst for highly efficient degradation of organic water pollutants, *J. Mater. Chem. A* 6 (2018) 4515–4524.
  - [71] M. Liu, W. Chen, Green synthesis of silver nanoclusters supported on carbon nanodots: enhanced photoluminescence and high catalytic activity for oxygen reduction reaction, *Nanoscale* 5 (2013) 12558–12564.
  - [72] X. Qin, W. Lu, G. Chang, Y. Luo, A.M. Asiri, A.O. Al-Youbi, X. Sun, Novel synthesis of Au nanoparticles using fluorescent carbon nitride dots as photocatalyst, *Gold Bull.* 45 (2012) 61–67.
  - [73] T. Liu, J.X. Dong, S.G. Liu, N. Li, S.M. Lin, Y.Z. Fan, J.L. Lei, H.Q. Luo, N.B. Li, Carbon quantum dots prepared with polyethyleneimine as both reducing agent and stabilizer for synthesis of Ag/CQDs composite for Hg(<sup>2+</sup>) ions detection, *J. Hazard Mater.* 322 (2017) 430–436.
  - [74] J. Wang, Y. Li, J. Ge, B.P. Zhang, W. Wan, Improving photocatalytic performance of ZnO via synergistic effects of Ag nanoparticles and graphene quantum dots, *Phys. Chem. Chem. Phys.* 17 (2015) 18645–18652.
  - [75] R. Liu, J. Liu, W. Kong, H. Huang, X. Han, X. Zhang, Y. Liu, Z. Kang, Adsorption dominant catalytic activity of a carbon dots stabilized gold nanoparticles system, *Dalton Trans.* 43 (2014) 10920–10929.
  - [76] X. Wang, Y. Long, Q. Wang, H. Zhang, X. Huang, R. Zhu, P. Teng, L. Liang, H. Zheng, Reduced state carbon dots as both reductant and stabilizer for the synthesis of gold nanoparticles, *Carbon* 64 (2013) 499–506.
  - [77] X. Liu, Y. Li, W. Xue, J. Ge, J. Wang, J. Sun, 3D nano-arrays of silver nanoparticles and graphene quantum dots with excellent surface-enhanced Raman scattering, *Mater. Sci. Technol.* 34 (2017) 679–687.
  - [78] L. Cao, S. Sahu, P. Anilkumar, C.E. Bunker, J. Xu, K.A.S. Fernando, P. Wang, E.A. Gulians, K.N. Tackett, Y.-P. Sun, Carbon Nanoparticles as Visible-Light Photocatalysts for Efficient CO<sub>2</sub> Conversion and Beyond, *J. Am. Chem. Soc.* 133 (2011) 4754–4757.
  - [79] J. Zhang, Y. Chen, J. Tan, H. Sang, L. Zhang, D. Yue, The synthesis of rhodium/carbon dots nanoparticles and its hydrogenation application, *Appl. Surf. Sci.* 396 (2017) 1138–1145.
  - [80] A. Jaiswal, P.K. Gautam, S.S. Ghosh, A. Chattopadhyay, Carbon dots mediated room-temperature synthesis of gold nanoparticles in poly(ethylene glycol), *J. Nanopart. Res.* 16 (2013).
  - [81] S. Mandani, B. Sharma, D. Dey, T.K. Sarma, Carbon nanodots as ligand exchange probes in Au@C-dot nanobeacons for fluorescent turn-on detection of biothiols, *Nanoscale* 7 (2015) 1802–1808.
  - [82] Q. Lu, Y. Liu, Y. Hou, H. Wang, Y. Zhang, S. Yao, Detection of thiocyanate through limiting growth of AuNPs with C-dots acting as reductant, *Analyst* 140 (2015) 7645–7649.
  - [83] P. Muthukumar, S.P. Anthony, Gold doping induced strong enhancement of carbon quantum dots fluorescence and oxygen evolution reaction catalytic activity of amorphous cobalt hydroxide, *New J. Chem.* 42 (2018) 18794–18801.
  - [84] C. Wang, K. Yang, X. Wei, S. Ding, F. Tian, F. Li, One-pot solvothermal synthesis of carbon dots/Ag nanoparticles/TiO<sub>2</sub> nanocomposites with enhanced photocatalytic performance, *Ceram. Int.* 44 (2018) 22481–22488.
  - [85] A. Meng, Q. Xu, K. Zhao, Z. Li, J. Liang, Q. Li, A highly selective and sensitive “on-off-on” fluorescent probe for detecting Hg(II) based on Au/N-doped carbon quantum dots, *Sens. Actuators, B* 255 (2018) 657–665.
  - [86] W. Li, Y. Liu, M. Wu, X. Feng, S.A.T. Redfern, Y. Shang, X. Yong, T. Feng, K. Wu, Z. Liu, B. Li, Z. Chen, J.S. Tse, S. Lu, B. Yang, Carbon-Quantum-Dots-Loaded Ruthenium Nanoparticles as an Efficient Electrocatalyst for Hydrogen Production in Alkaline Media, *Adv. Mater.* 30 (2018) e1800676.
  - [87] B. Han, Y. Li, X. Hu, Q. Yan, J. Jiang, M. Yu, T. Peng, G. He, Paper-based visual detection of silver ions and l-cysteine with a dual-emissive nanosystem of carbon quantum dots and gold nanoclusters, *Anal. Methods* 10 (2018) 3945–3950.
  - [88] W.-J. Niu, D. Shan, R.-H. Zhu, S.-Y. Deng, S. Cosnier, X.-J. Zhang, Dumbbell-shaped carbon quantum dots/AuNCs nanohybrid as an efficient ratiometric fluorescent probe for sensing cadmium (II) ions and l-ascorbic acid, *Carbon* 96 (2016) 1034–1042.
  - [89] R. Duarah, N. Karak, Hyperbranched Polyurethane/Palladium-Reduced Carbon Dot Nanocomposite: An Efficient and Reusable Mesoporous Catalyst for Visible-Light-Driven C–C Coupling Reactions, *Ind. Eng. Chem. Res.* 58 (2019) 16307–16319.
  - [90] L. Li, T. Zhang, J. Lü, C. Lü, A facile construction of Au nanoparticles stabilized by thermo-responsive polymer-tethered carbon dots for enhanced catalytic performance, *Appl. Surf. Sci.* 454 (2018) 181–191.
  - [91] J. Jin, S. Zhu, Y. Song, H. Zhao, Z. Zhang, Y. Guo, J. Li, W. Song, B. Yang, B. Zhao, Precisely Controllable Core-Shell Ag@Carbon Dots Nanoparticles: Application to in Situ Super-Sensitive Monitoring of Catalytic Reactions, *ACS Appl. Mater. Interfaces* 8 (2016) 27956–27965.
  - [92] T.R. Kiran, M.L. Yola, A. Atar, Electrochemical Sensor Based on Au@nitrogen-Doped Carbon Quantum Dots@Ag Core-Shell Composite Including Molecular Imprinted Polymer for Metobromuron Recognition, *J. Electrochem. Soc.* 166 (2019) H691–H697.
  - [93] M.K. Mahto, D. Samanta, S. Konar, H. Kalita, A. Pathak, N. S. doped carbon dots—Plasmonic Au nanocomposites for visible-light photocatalytic reduction of nitroaromatics, *J. Mater. Res.* 33 (2018) 3906–3916.
  - [94] F. Sun, H. Maimaiti, Y.-E. Liu, A. Awati, Preparation and photocatalytic CO<sub>2</sub> reduction performance of silver nanoparticles coated with coal-based carbon dots, *Int. J. Energy Res.* 42 (2018) 4458–4469.
  - [95] J. Yang, C. Luo, S. He, J. Li, B. Meng, D. Zhang, Z. Xue, X. Zhou, X. Lu, Synthesis of three-dimensional Au-graphene quantum dots@Pt core-shell dendritic nanoparticles for enhanced methanol electro-oxidation, *Nanotechnology* 30 (2019) 495706.
  - [96] X. Liu, D. Huang, C. Lai, G. Zeng, L. Qin, H. Wang, H. Yi, B. Li, S. Liu, M. Zhang, R. Deng, Y. Fu, L. Li, W. Xue, S. Chen, Recent advances in covalent organic frameworks (COFs) as a smart sensing material, *Chem. Soc. Rev.* (2019).
  - [97] C. Lai, X. Liu, L. Qin, C. Zhang, G. Zeng, D. Huang, M. Cheng, P. Xu, H. Yi, D. Huang, Chitosan-wrapped gold nanoparticles for hydrogen-bonding recognition and colorimetric determination of the antibiotic kanamycin, *Microchim. Acta* 184 (2017) 2097–2105.
  - [98] B.P. Chaplin, M. Reinhard, W.F. Schneider, C. Schüth, J.R. Shapley, T.J. Strathmann, C.J. Werth, Critical Review of Pd-Based Catalytic Treatment of Priority Contaminants in Water, *Environ. Sci. Technol.* 46 (2012) 3655–3670.
  - [99] J. He, C. Lai, L. Qin, B. Li, S. Liu, L. Jiao, Y. Fu, D. Huang, L. Li, M. Zhang, X. Liu, H. Yi, L. Chen, Z. Li, Strategy to improve gold nanoparticles loading efficiency on defect-free high silica ZSM-5 zeolite for the reduction of nitrophenols, *Chemosphere* 256 (2020) 127083.
  - [100] H. Yi, L. Qin, D. Huang, G. Zeng, C. Lai, X. Liu, B. Li, H. Wang, C. Zhou, F. Huang, S. Liu, X. Guo, Nano-structured bismuth tungstate with controlled morphology: Fabrication, modification, environmental application and mechanism insight, *Chem. Eng. J.* 358 (2019) 480–496.
  - [101] P. Mondal, K. Ghosal, S.K. Bhattacharyya, M. Das, A. Bera, D. Ganguly, P. Kumar, J. Dwivedi, R.K. Gupta, A.A. Martí, B.K. Gupta, S. Maiti, Formation of a gold–carbon dot nanocomposite with superior catalytic ability for the reduction of aromatic nitro groups in water, *RSC Adv.* 4 (2014) 25863–25866.
  - [102] Y. Yang, H. Duan, S. Xia, C. Lü, Construction of a thermo-responsive copolymer-stabilized Fe<sub>3</sub>O<sub>4</sub>@CD@PdNP hybrid and its application in catalytic reduction, *Polym. Chem.* 11 (2020) 1177–1187.
  - [103] W. Lv, Y. Ju, Y. Chen, X. Chen, In situ synthesis of gold nanoparticles on N-doped graphene quantum dots for highly efficient catalytic degradation of nitrophenol, *Int. J. Hydrogen Energy* 43 (2018) 10334–10340.
  - [104] C. Lu, Q. Zhu, X. Zhang, H. Ji, Y. Zhou, H. Wang, Q. Liu, J. Nie, W. Han, X. Li, Decoration of Pd Nanoparticles with N and S Doped Carbon Quantum Dots as a Robust Catalyst for the Chemoselective Hydrogenation Reaction, *ACS Sustainable Chem. Eng.* 7 (2019) 8542–8553.
  - [105] J.B. Essner, C.H. Laber, G.A. Baker, Carbon dot reduced bimetallic nanoparticles: size and surface plasmon resonance tunability for enhanced catalytic applications, *J. Mater. Chem. A* 3 (2015) 16354–16360.
  - [106] P. Fageria, S. Uppala, R. Nazir, S. Gangopadhyay, C.H. Chang, M. Basu, S. Pande, Synthesis of Monometallic (Au and Pd) and Bimetallic (AuPd) Nanoparticles Using Carbon Nitride (C<sub>3</sub>N<sub>4</sub>) Quantum Dots via the Photochemical Route for Nitrophenol Reduction, *Langmuir* 32 (2016) 10054–10064.
  - [107] M. Zhang, C. Lai, B. Li, D. Huang, G. Zeng, P. Xu, L. Qin, S. Liu, X. Liu, H. Yi, M. Li, C. Chu, Z. Chen, Rational design 2D/2D BiOBr/CDs/g-C<sub>3</sub>N<sub>4</sub> Z-scheme heterojunction photocatalyst with carbon dots as solid-state electron mediators for enhanced visible and NIR photocatalytic activity: Kinetics, intermediates, and mechanism insight, *J. Catal.* 369 (2019) 469–481.
  - [108] Y. Yang, C. Zhang, C. Lai, G. Zeng, D. Huang, M. Cheng, J. Wang, F. Chen, C. Zhou, W. Xiong, BiOX (X = Cl, Br, I) photocatalytic nanomaterials: applications for fuels and environmental management, *Adv. Colloid Interface Sci.* 254 (2018) 76–93.
  - [109] H. Yi, M. Yan, D. Huang, G. Zeng, C. Lai, M. Li, X. Huo, L. Qin, S. Liu, X. Liu, Synergistic effect of artificial enzyme and 2D nano-structured Bi<sub>2</sub>WO<sub>6</sub> for eco-friendly and efficient biomimetic photocatalysis, *Appl. Catal. B* 250 (2019) 52–62.
  - [110] L. Li, C. Lai, F. Huang, M. Cheng, G. Zeng, D. Huang, B. Li, S. Liu, M. Zhang, L. Qin, M. Li, J. He, Y. Zhang, L. Chen, Degradation of naphthalene with magnetic bio-char activate hydrogen peroxide: Synergism of bio-char and Fe–Mn binary oxides, *Water Res.* 160 (2019) 238–248.
  - [111] W. Wang, Z. Zeng, G. Zeng, C. Zhang, R. Xiao, C. Zhou, W. Xiong, Y. Yang, L. Lei, Y. Liu, D. Huang, M. Cheng, Y. Zhang, Y. Fu, H. Luo, Y. Zhou, Sulfur doped carbon quantum dots loaded hollow tubular g-C<sub>3</sub>N<sub>4</sub> as novel photocatalyst for destruction of *Escherichia coli* and tetracycline degradation under visible light, *Chem. Eng. J.* 378 (2019) 122132.
  - [112] H. Yi, M. Jiang, D. Huang, G. Zeng, C. Lai, L. Qin, C. Zhou, B. Li, X. Liu, M. Cheng, W. Xue, P. Xu, C. Zhang, Advanced photocatalytic Fenton-like process over biomimetic hemin-Bi<sub>2</sub>WO<sub>6</sub> with enhanced pH, *J. Taiwan Inst. Chem. Eng.* 93 (2018) 184–192.
  - [113] C. Feng, Y. Deng, L. Tang, G. Zeng, J. Wang, J. Yu, Y. Liu, B. Peng, H. Feng, J. Wang, Core-shell Ag<sub>2</sub>CrO<sub>4</sub>/N-GQDs@g-C<sub>3</sub>N<sub>4</sub> composites with anti-photocorrosion performance for enhanced full-spectrum-light photocatalytic activities, *Appl. Catal. B* 239 (2018) 525–536.
  - [114] F. Wang, Y. Wang, Y. Feng, Y. Zeng, Z. Xie, Q. Zhang, Y. Su, P. Chen, Y. Liu, K. Yao, W. Lv, G. Liu, Novel ternary photocatalyst of single atom-dispersed silver and carbon quantum dots co-loaded with ultrathin g-C<sub>3</sub>N<sub>4</sub> for broad spectrum photocatalytic degradation of naproxen, *Appl. Catal. B* 221 (2018) 510–520.
  - [115] Y. Yang, G. Zeng, D. Huang, C. Zhang, D. He, C. Zhou, W. Wang, W. Xiong, X. Li, B. Li, W. Dong, Y. Zhou, Molecular engineering of polymeric carbon nitride for highly efficient photocatalytic oxytetracycline degradation and H<sub>2</sub>O<sub>2</sub> production, *Appl. Catal. B* 272 (2020) 118970.
  - [116] W. Wang, Q. Niu, G. Zeng, C. Zhang, D. Huang, B. Shao, C. Zhou, Y. Yang, Y. Liu, H. Guo, W. Xiong, L. Lei, S. Liu, H. Yi, S. Chen, X. Tang, 1D porous tubular g-C<sub>3</sub>N<sub>4</sub> capture black phosphorus quantum dots as 1D/0D metal-free photocatalysts for oxytetracycline hydrochloride degradation and hexavalent chromium reduction, *Appl. Catal. B* 273 (2020) 119051.



- [117] Z. Mohammadpour, A. Safavi, S.H. Abdollahi, Chlorine triggered de-alloying of AuAg@Carbon nanodots: Towards fabrication of a dual signalling assay combining the plasmonic property of bimetallic alloy nanoparticles and photoluminescence of carbon nanodots, *Anal Chim Acta* 959 (2017) 74–82.
- [118] K. Aslan, M. Wu, J.R. Lakowicz, C.D. Geddes, Fluorescent Core–Shell Ag@SiO<sub>2</sub> Nanocomposites for Metal-Enhanced Fluorescence and Single Nanoparticle Sensing Platforms, *J. Am. Chem. Soc.* 129 (2007) 1524–1525.
- [119] Y. Zhou, Z. Ma, A novel fluorescence enhanced route to detect copper(II) by click chemistry-catalyzed connection of Au@SiO<sub>2</sub> and carbon dots, *Sens. Actuators, B* 233 (2016) 426–430.
- [120] W. Liu, X. Wang, Y. Wang, J. Li, D. Shen, Q. Kang, L. Chen, Ratiometric fluorescence sensor based on dithiothreitol modified carbon dots-gold nanoclusters for the sensitive detection of mercury ions in water samples, *Sens. Actuators, B* 262 (2018) 810–817.
- [121] L. Yu, L. Zhang, G. Ren, S. Li, B. Zhu, F. Chai, F. Qu, C. Wang, Z. Su, Multicolorful fluorescent-nanoprobe composed of Au nanocluster and carbon dots for colorimetric and fluorescent sensing Hg<sup>2+</sup> and Cr<sup>6+</sup>, *Sens. Actuators, B* 262 (2018) 678–686.
- [122] Y. Yan, H. Yu, K. Zhang, M. Sun, Y. Zhang, X. Wang, S. Wang, Dual-emissive nanohybrid of carbon dots and gold nanoclusters for sensitive determination of mercuric ions, *Nano Res.* 9 (2016) 2088–2096.
- [123] H. Lu, S. Quan, S. Xu, Highly Sensitive Ratiometric Fluorescent Sensor for Trinitrotoluene Based on the Inner Filter Effect between Gold Nanoparticles and Fluorescent Nanoparticles, *J. Agric Food Chem* 65 (2017) 9807–9814.
- [124] K.E. Sapsford, L. Berti, I.L. Medintz, Materials for fluorescence resonance energy transfer analysis: beyond traditional donor–acceptor combinations, *Angew. Chem. Int. Ed.* 45 (2006) 4562–4589.
- [125] X. Wu, Y. Song, X. Yan, C. Zhu, Y. Ma, D. Du, Y. Lin, Carbon quantum dots as fluorescence resonance energy transfer sensors for organophosphate pesticides determination, *Biosens Bioelectron* 94 (2017) 292–297.
- [126] Y. Yang, D. Huo, H. Wu, X. Wang, J. Yang, M. Bian, Y. Ma, C. Hou, N. P-doped carbon quantum dots as a fluorescent sensing platform for carbendazim detection based on fluorescence resonance energy transfer, *Sens. Actuators, B* 274 (2018) 296–303.
- [127] B. Shi, Y. Su, L. Zhang, M. Huang, R. Liu, S. Zhao, Nitrogen and Phosphorus Co-Doped Carbon Nanodots as a Novel Fluorescent Probe for Highly Sensitive Detection of Fe<sup>3+</sup> in Human Serum and Living Cells, *ACS Appl. Mater. Interfaces* 8 (2016) 10717–10725.
- [128] F. Wang, J. Sun, Y. Lu, X. Zhang, P. Song, Y. Liu, Dispersion-aggregation-dispersion colorimetric detection for mercury ions based on an assembly of gold nanoparticles and carbon nanodots, *Analyst* 143 (2018) 4741–4746.
- [129] M. Shamsipur, A. Safavi, Z. Mohammadpour, R. Ahmadi, Highly selective aggregation assay for visual detection of mercury ion based on competitive binding of sulfur-doped carbon nanodots to gold nanoparticles and mercury ions, *Microchim. Acta* 183 (2016) 2327–2335.
- [130] D. Zhao, C. Chen, L. Lu, F. Yang, X. Yang, A dual-mode colorimetric and fluorometric “light on” sensor for thiocyanate based on fluorescent carbon dots and unmodified gold nanoparticles, *Analyst* 140 (2015) 8157–8164.
- [131] S. Zhang, X. Liu, N. Huang, Q. Lu, M. Liu, H. Li, Y. Zhang, S. Yao, Sensitive detection of hydrogen peroxide and nitrite based on silver/carbon nanocomposite synthesized by carbon dots as reductant via one step method, *Electrochim. Acta* 211 (2016) 36–43.
- [132] Y. Zuo, J. Xu, F. Jiang, X. Duan, L. Lu, G. Ye, C. Li, Y. Yu, Utilization of AuNPs dotted S-doped carbon nanoflakes as electrochemical sensing platform for simultaneous determination of Cu (II) and Hg (II), *J. Electroanal. Chem.* 794 (2017) 71–77.
- [133] Z. Zhuang, H. Lin, X. Zhang, F. Qiu, H. Yang, A glassy carbon electrode modified with carbon dots and gold nanoparticles for enhanced electrocatalytic oxidation and detection of nitrite, *Microchim. Acta* 183 (2016) 2807–2814.
- [134] S. Yang, Y. Li, S. Wang, M. Wang, M. Chu, B. Xia, Advances in the use of carbonaceous materials for the electrochemical determination of persistent organic pollutants, A review, *Mikrochim. Acta* 185 (2018) 112.
- [135] Y.-Y. Lu, N.-L. Li, L.-P. Jia, R.-N. Ma, W.-L. Jia, X.-Q. Tao, H. Cui, H.-S. Wang, The synthesis of Ag@CQDs composite and its electrochemiluminescence application for the highly selective and sensitive detection of chloramide, *J. Electroanal. Chem.* 781 (2016) 114–119.
- [136] Z.X. Wang, C.L. Zheng, Q.L. Li, S.N. Ding, Electrochemiluminescence of a nanoAg-carbon nanodot composite and its application to detect sulfide ions, *Analyst* 139 (2014) 1751–1755.
- [137] X. Liu, D. Huang, C. Lai, G. Zeng, L. Qin, C. Zhang, H. Yi, B. Li, R. Deng, S. Liu, Y. Zhang, Recent advances in sensors for tetracycline antibiotics and their applications, *TrAC, Trends Anal. Chem.* 109 (2018) 260–274.
- [138] M. Roushani, K. Ghanbari, S. Jafar Hoseini, Designing an electrochemical aptasensor based on immobilization of the aptamer onto nanocomposite for detection of the streptomycin antibiotic, *Microchem. J.* 141 (2018) 96–103.
- [139] C. Xiong, W. Liang, H. Wang, Y. Zheng, Y. Zhuo, Y. Chai, R. Yuan, In situ electropolymerization of nitrogen doped carbon dots and their application in an electrochemiluminescence biosensor for the detection of intracellular lead ions, *Chem Commun (Camb)* 52 (2016) 5589–5592.
- [140] B. Li, C. Lai, G. Zeng, D. Huang, L. Qin, M. Zhang, M. Cheng, X. Liu, H. Yi, C. Zhou, F. Huang, S. Liu, Y. Fu, Black Phosphorus, a Rising Star 2D Nanomaterial in the Post-Graphene Era: Synthesis, Properties, Modifications, and Photocatalysis Applications, *Small* 15 (2019) e1804565.
- [141] A. Fujishima, K. Honda, Electrochemical Photolysis of Water at a Semiconductor Electrode, *Nature* 238 (1972) 37–38.
- [142] T.-F. Yeh, C.-Y. Teng, S.-J. Chen, H. Teng, Nitrogen-Doped Graphene Oxide Quantum Dots as Photocatalysts for Overall Water-Splitting under Visible Light Illumination, *Adv. Mater.* 26 (2014) 3297–3303.
- [143] C. Zhou, P. Xu, C. Lai, C. Zhang, G. Zeng, D. Huang, M. Cheng, L. Hu, W. Xiong, X. Wen, L. Qin, J. Yuan, W. Wang, Rational design of graphitic carbon nitride copolymers by molecular doping for visible-light-driven degradation of aqueous sulfamethazine and hydrogen evolution, *Chem. Eng. J.* 359 (2019) 186–196.
- [144] P. Yang, J. Zhao, J. Wang, H. Cui, L. Li, Z. Zhu, Multifunctional Nitrogen-Doped Carbon Nanodots for Photoluminescence, Sensor, and Visible-Light-Induced H<sub>2</sub> Production, *ChemPhysChem* 16 (2015) 3058–3063.
- [145] Q. Li, C. Cui, H. Meng, J. Yu, Visible-light photocatalytic hydrogen production activity of ZnIn<sub>2</sub>S<sub>4</sub> microspheres using carbon quantum dots and platinum as dual co-catalysts, *Chem Asian J* 9 (2014) 1766–1770.
- [146] B.S. Nguyen, Y.K. Xiao, C.Y. Shih, V.C. Nguyen, W.Y. Chou, H. Teng, Electronic structure manipulation of graphene dots for effective hydrogen evolution from photocatalytic water decomposition, *Nanoscale* 10 (2018) 10721–10730.
- [147] T.-F. Yeh, S.-J. Chen, H. Teng, Synergistic effect of oxygen and nitrogen functionalities for graphene-based quantum dots used in photocatalytic H<sub>2</sub> production from water decomposition, *Nano Energy* 12 (2015) 476–485.
- [148] J. Qin, H. Zeng, Photocatalysts fabricated by depositing plasmonic Ag nanoparticles on carbon quantum dots/graphitic carbon nitride for broad spectrum photocatalytic hydrogen generation, *Appl. Catal. B* 209 (2017) 161–173.
- [149] S. Sahu, Y. Liu, P. Wang, C.E. Bunker, K.A. Fernando, W.K. Lewis, E.A. Gulians, F. Yang, J. Wang, Y.P. Sun, Visible-light photoconversion of carbon dioxide into organic acids in an aqueous solution of carbon dots, *Langmuir* 30 (2014) 8631–8636.
- [150] S. Sahu, L. Cao, M.J. Meziani, C.E. Bunker, K.A. Shiral Fernando, P. Wang, Y.-P. Sun, Carbon dioxide photoconversion driven by visible-light excitation of small carbon nanoparticles in various configurations, *Chem. Phys. Lett.* 634 (2015) 122–128.
- [151] D. Pan, X. Li, A. Zhang, Platinum assisted by carbon quantum dots for methanol electro-oxidation, *Appl. Surf. Sci.* 427 (2018) 715–723.
- [152] P. Luo, L. Jiang, W. Zhang, X. Guan, Graphene quantum dots/Au hybrid nanoparticles as electrocatalyst for hydrogen evolution reaction, *Chem. Phys. Lett.* 641 (2015) 29–32.
- [153] Q. Dang, F. Liao, Y. Sun, S. Zhang, H. Huang, W. Shen, Z. Kang, Y. Shi, M. Shao, Rhodium/silicon quantum dot/carbon quantum dot composites as highly efficient electrocatalysts for hydrogen evolution reaction with Pt-like performance, *Electrochim. Acta* 299 (2019) 828–834.
- [154] C.P. Deming, R. Mercado, V. Gadiraaju, S.W. Sweeney, M. Khan, S. Chen, Graphene Quantum Dots-Supported Palladium Nanoparticles for Efficient Electrocatalytic Reduction of Oxygen in Alkaline Media, *ACS Sustainable Chem. Eng.* 3 (2015) 3315–3323.
- [155] L. Wang, C. Hu, Y. Zhao, Y. Hu, F. Zhao, N. Chen, L. Qu, A dually spontaneous reduction and assembly strategy for hybrid capsules of graphene quantum dots with platinum–copper nanoparticles for enhanced oxygen reduction reaction, *Carbon* 74 (2014) 170–179.
- [156] G. He, Y. Song, K. Liu, A. Walter, S. Chen, S. Chen, Oxygen Reduction Catalyzed by Platinum Nanoparticles Supported on Graphene Quantum Dots, *ACS Catal.* 3 (2013) 831–838.
- [157] A. Zhang, X. Li, Y. He, Platinum/nitrogen-doped carbon nanoparticles synthesized in nitrogen-doped carbon quantum dots aqueous solution for methanol electro-oxidation, *Electrochim. Acta* 213 (2016) 332–340.
- [158] L. Chen, Y. Peng, J.-E. Lu, N. Wang, P. Hu, B. Lu, S. Chen, Platinum nanoparticles encapsulated in nitrogen-doped graphene quantum dots: Enhanced electrocatalytic reduction of oxygen by nitrogen dopants, *Int. J. Hydrogen Energy* 42 (2017) 29192–29200.
- [159] K. Kakaei, High efficiency platinum nanoparticles based on carbon quantum dot and its application for oxygen reduction reaction, *Int. J. Hydrogen Energy* 42 (2017) 11605–11613.
- [160] D.-W. Wang, D. Su, Heterogeneous nanocarbon materials for oxygen reduction reaction, *Energy Environ. Sci.* 7 (2014) 576–591.
- [161] J.-J. Lv, J. Zhao, H. Fang, L.-P. Jiang, L.-L. Li, J. Ma, J.-J. Zhu, Incorporating Nitrogen-Doped Graphene Quantum Dots and Ni<sub>3</sub>S<sub>2</sub> Nanosheets: A Synergistic Electrocatalyst with Highly Enhanced Activity for Overall Water Splitting, *Small* 13 (2017) 1700264.
- [162] Z. Lei, S. Xu, J. Wan, P. Wu, Facile synthesis of N-rich carbon quantum dots by spontaneous polymerization and incision of solvents as efficient bioimaging probes and advanced electrocatalysts for oxygen reduction reaction, *Nanoscale* 8 (2016) 2219–2226.
- [163] J. Cao, Y. Hu, L. Chen, J. Xu, Z. Chen, Nitrogen-doped carbon quantum dot/graphene hybrid nanocomposite as an efficient catalyst support for the oxygen reduction reaction, *Int. J. Hydrogen Energy* 42 (2017) 2931–2942.
- [164] C.P. Deming, R. Mercado, J.E. Lu, V. Gadiraaju, M. Khan, S. Chen, Oxygen Electrocatalysis Catalyzed by Palladium Nanoparticles Supported on Nitrogen-Doped Graphene Quantum Dots: Impacts of Nitrogen Dopants, *ACS Sustainable Chem. Eng.* 4 (2016) 6580–6589.
- [165] J.-J. Zhang, X.-L. Sui, L. Zhao, L.-M. Zhang, D.-M. Gu, Z.-B. Wang, Effect of N-doped carbon quantum dots/multiwall-carbon nanotube composite support on Pt catalytic performance for methanol electrooxidation, *RSC Adv.* 6 (2016) 67096–67101.
- [166] T.-Z. Hong, Q. Xue, Z.-Y. Yang, Y.-P. Dong, Great-enhanced performance of Pt nanoparticles by the unique carbon quantum dot/reduced graphene oxide hybrid supports towards methanol electrochemical oxidation, *J. Power Sources* 303 (2016) 109–117.
- [167] A. Bora, K. Mohan, S. Doley, P. Goswami, S.K. Dolui, Broadening the sunlight response region with carbon dot sensitized TiO<sub>2</sub> as a support for a Pt catalyst in the

- methanol oxidation reaction, Catal. Sci. Technol. 8 (2018) 4180–4192.
- [168] A. Thakur, P. Kumar, D. Kaur, N. Devunuri, R.K. Sinha, P. Devi, TiO<sub>2</sub> nanofibres decorated with green-synthesized PAu/Ag@CQDs for the efficient photocatalytic degradation of organic dyes and pharmaceutical drugs, RSC Adv. 10 (2020) 8941–8948.
- [169] G. Sharma, A. Kumar, M. Naushad, A. Kumar, A.a.H. Al-Muhtaseb, P. Dhiman, A.A. Ghfar, F.J. Stadler, M.R. Khan, Photoremediation of toxic dye from aqueous environment using monometallic and bimetallic quantum dots based nano-composites, J. Cleaner Prod. 172 (2018) 2919–2930.
- [170] Y. Yang, X. Xing, T. Zou, Z. Wang, R. Zhao, P. Hong, S. Peng, X. Zhang, Y. Wang, A novel and sensitive ratiometric fluorescence assay for carbendazim based on N-doped carbon quantum dots and gold nanocluster nanohybrid, J. Hazard. Mater. 386 (2020) 121958.
- [171] Z. Zhang, Z. Zhang, H. Liu, X. Mao, W. Liu, S. Zhang, Z. Nie, X. Lu, Ultratrace and robust visual sensor of Cd<sup>2+</sup> ions based on the size-dependent optical properties of Au@g-CNQDs nanoparticles in mice models, Biosens. Bioelectron. 103 (2018) 87–93.